

NAVAL POSTGRADUATE SCHOOL Monterey, California



THESIS

METHODS OF GENERATING LOW REDUNDANCY
DIRECTION FINDING ARRAY CONFIGURATIONS

by

Dafer R. AL-Jalahma

December 1994

Thesis Advisor:

David C. Jenn

Approved for public release; distribution is unlimited.

19950323 040

REPORT DOCUMENTATION PAGE

Form Approved
OMB No. 0704-0188

Public reporting burden for this collection of information is estimated to average 1 hour per response, including the time for reviewing instructions, searching existing data sources, gathering and maintaining the data needed, and completing and reviewing the collection of information. Send comments regarding this burden estimate or any other aspect of this collection of information, including suggestions for reducing the burden, to Washington Headquarters Services, Directorate for Information Operations and Reports, 1215 Jefferson Davis Highway, Suite 1204, Arlington, VA 22202-4302, and to the Office of Management and Budget, Paperwork Reduction Project (0704-0188), Washington, DC 20503.

| | | | | |
|---|--|---|---|--|
| 1. AGENCY USE ONLY (Leave blank) | | 2. REPORT DATE December, 1994 | 3. REPORT TYPE AND DATES COVERED Master's Thesis | |
| 4. TITLE AND SUBTITLE METHODS OF GENERATING LOW REDUNDANCY DIRECTION FINDING ARRAY CONFIGURATIONS | | | 5. FUNDING NUMBERS | |
| 6. AUTHOR(S) Dafer R. AL-Jalahma | | | | |
| 7. PERFORMING ORGANIZATION NAME(S) AND ADDRESS(S) Naval Postgraduate School Monterey, Ca. 93943-5000 | | | 8. PERFORMING ORGANIZATION REPORT NUMBER | |
| 9. SPONSORING / MONITORING AGENCY NAME(S) AND ADDRESS(S) | | | 10. SPONSORING / MONITORING AGENCY REPORT NUMBER | |
| 11. SUPPLEMENTARY NOTES The views expressed in this thesis are those of the author and do not reflect the official policy or position of the Department of Defense or the U.S. Government. | | | | |
| 12a. DISTRIBUTION / AVAILABILITY STATEMENT Approved for public release; distribution unlimited | | | 12b. DISTRIBUTION CODE | |
| 13. ABSTRACT (Maximum 200 words) Standard uniformly spaced arrays are used to obtain direction information about jammers and other interference signals. In conventional systems the number of sources that can be identified by an array of N elements is $N-1$. Minimum redundancy arrays have the ability to handle more than $N-1$ interferers (up to $N(N-1)/2$) with N elements or less. They require the use of nonuniformly spaced array elements. The existing method for finding the element locations for an optimum minimum redundancy array (MRA) is restricted by its processing time. For a 10 element array with an array length of $36d$ (d is the fundamental element spacing, typically one half wavelength), the number of possibilities is much greater than 6×10^{10} . Thus, even with today's fast computers, finding the optimum MRA for a large arrays is not practical. A new element placement procedure is investigated based on the residue number system (RNS). The element locations are obtained from simple modulo computations, and by varying the base of the number systems, different configurations are generated. The residue array does not achieve the minimum redundancy of the optimum array, but has significantly lower redundancy than the conventional periodic array. The advantages and disadvantages of both methods are investigated, and the array response of each is compared. | | | | |
| 14. SUBJECT TERMS Minimum Redundancy Arrays | | | 15. NUMBER OF PAGES 91 | |
| | | | 16. PRICE CODE | |
| 17. SECURITY CLASSIFICATION OF REPORT UNCLASSIFIED | 18. SECURITY CLASSIFICATION OF THIS PAGE UNCLASSIFIED | 19. SECURITY CLASSIFICATION OF ABSTRACT UNCLASSIFIED | 20. LIMITATION OF ABSTRACT UL | |

Approved for public release; distribution is unlimited

METHODS OF GENERATING LOW REDUNDANCY
DIRECTION FINDING ARRAY CONFIGURATIONS
by

Dafer R. AL-Jalahma
Captain, Bahrain Air Force
B. S., Plymouth University, 1986

Submitted in partial fulfillment
of the requirements for the degree of

MASTER OF SCIENCE IN ELECTRICAL ENGINEERING
and
MASTER OF SCIENCE IN SYSTEMS ENGINEERING

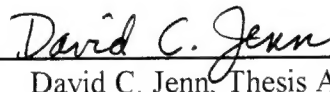
from the
NAVAL POSTGRADUATE SCHOOL
December 1994

Author:



Dafer R. AL-Jalahma

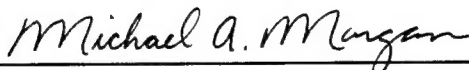
Approved by:




David C. Jenn, Thesis Advisor



Phillip E. Pace, Second Reader



Michael A. Morgan, Chairman,
Department of Electrical and Computer Engineering



Frederic H. Levien, Chairman,
Electronic Warfare Academic Group

| | |
|--------------------|-------------------------------------|
| Accession For | |
| NTIS CRA&I | <input checked="" type="checkbox"/> |
| DTIC TAB | <input type="checkbox"/> |
| Unannounced | <input type="checkbox"/> |
| Justification | |
| By _____ | |
| Distribution / | |
| Availability Codes | |
| Dist | Avail and/or Special |
| A-1 | |

ABSTRACT

Standard uniformly spaced arrays are used to obtain direction information about jammers and other interference signals. In conventional systems the number of sources that can be identified by an array of N elements is $N-1$. Minimum redundancy arrays have the ability to handle more than $N-1$ interferers (up to $N(N-1)/2$) with N elements or less. They require the use of nonuniformly spaced array elements.

The existing method for finding the element locations for an optimum minimum redundancy array (MRA) is restricted by its processing time. For a 10 element array with an array length of $36d$ (d is the fundamental element spacing, typically one half wavelength), the number of possibilities is much greater than 6×10^{10} . Thus, even with today's fast computers, finding the optimum MRA for a large arrays is not practical. A new element placement procedure is investigated based on the residue number system (RNS). The element locations are obtained from simple modulo computations, and by varying the base of the number systems, different configurations are generated. The residue array does not achieve the minimum redundancy of the optimum array, but has significantly lower redundancy than the conventional periodic array. The advantages and disadvantages of both methods are investigated, and the array response of each is compared

TABLE OF CONTENTS

| | |
|---|----|
| I. INTRODUCTION | 1 |
| II. ARRAY BEAMFORMING | 5 |
| A. INTRODUCTION | 5 |
| B. ARRAY FACTOR FOR AN EQUALLY SPACED ARRAY | 6 |
| C. DEGREES OF FREEDOM | 8 |
| D. COVARIANCE MATRIX OF AN ARRAY | 8 |
| E. MATRIX DECOMPOSITION FOR DIRECTION OF ARRIVAL | 12 |
| F. METHODS FOR IMPROVED SPATIAL SPECTRUM ESTIMATION | 16 |
| III. MINIMUM-REDUNDANCY LINEAR ARRAYS | 19 |
| A. INTRODUCTION | 19 |
| B. OPTIMUM MINIMUM-REDUNDANCY ARRAYS | 21 |
| 1. Restricted Case vs General Case | 25 |
| 2. Advantage and Disadvantage of MRA's | 27 |
| C. THE RESIDUE NUMBER SYSTEM (RNS) | 28 |
| 1. Introduction | 28 |
| 2. RNS Encoding for Arrays | 29 |
| 3. Incorporation of RNS into Array Design | 31 |
| IV. SIMULATION RESULTS | 35 |
| A. DATA | 35 |
| B. SUMMARY OF SIMULATION RESULTS | 56 |

| | |
|---|----|
| V. CONCLUSIONS AND RECOMMENDATIONS | 57 |
| APPENDIX A. COMPUTER CODES | 59 |
| APPENDIX B. RESIDUAL ARRAY PERFORMANCE DATA | 69 |
| LIST OF REFERENCES | 73 |
| INITIAL DISTRIBUTION LIST | 75 |

LIST OF FIGURES

| | | |
|-----|--|----|
| 1. | Far-field geometry of N -element array of isotropic sources positioned along the z -axis (From [4]) | 7 |
| 2. | An N -element adaptive array | 9 |
| 3. | Conventional equally spaced array with $L = 6d$, $N = 6$ | 14 |
| 4. | Conventional processing scheme for a C-array with $L = 6d$, $N = 4$ | 15 |
| 5. | The improved spatial spectrum estimation using the augmented matrix for a C-array with $L = 6d$ and $N = 4$ | 18 |
| 6. | (a) Grating interferometer with $N = 8$. (b) Spatial sensitivity diagram for the grating interferometer | 20 |
| 7. | The four lowest N zero-redundancy linear arrays and their spatial sensitivity diagrams (From [7]) | 21 |
| 8. | (a) Compound grating interferometer with branching feeds and a single correlation detector. (b) Modified compound grating interferometer. | 23 |
| 9. | The redundancy R_r vs the number of elements N with the length fixed at $L=19d$.. | 24 |
| 10. | The two restricted minimum-redundancy eight-element arrays. | 25 |
| 11. | The general minimum-redundancy eight-element arrays | 25 |
| 12. | The RNS antenna response for $N = 9$, $L = 12$ | 36 |
| 13. | The optimum antenna response for $N = 9$, $L = 12$ | 37 |
| 14. | The RNS antenna response for $N = 9$, $L = 12$ and $N_{\max} = 10$ | 38 |
| 15. | The RNS antenna response for $N = 13$, $L = 18$ | 40 |
| 16. | The optimum antenna response for $N = 13$, $L = 18$ | 41 |
| 17. | The RNS antenna response for $N = 13$, $L = 18$ and $N_{\max} = 16$ | 42 |
| 18. | The RNS antenna response for $N = 17$, $L = 24$ | 44 |
| 19. | The optimum antenna response for $N = 17$, $L = 24$ | 45 |
| 20. | The RNS antenna response for $N = 17$, $L = 24$ and $N_{\max} = 22$ | 46 |
| 21. | The RNS antenna response for $N = 23$, $L = 30$ | 48 |
| 22. | The optimum antenna response for $N = 23$, $L = 30$ | 49 |

| | | |
|-----|--|----|
| 23. | The RNS antenna response for $N = 23$, $L = 30$ and $N_{\max} = 28$ | 50 |
| 24. | The RNS antenna response for $N = 19$, $L = 36$ | 53 |
| 25. | The optimum antenna response for $N = 19$, $L = 36$ | 54 |
| 26. | The RNS antenna response for $N = 19$, $L = 36$ and $N_{\max} = 30$ | 55 |

LIST OF TABLES

| | | |
|-----|---|----|
| 1. | Some minimum-redundancy array configurations (After [3]) | 26 |
| 2. | An example to illustrate the encoding procedure for $(N_1 = 3, N_2 = 4, N_3 = 5)$ | 30 |
| 3. | Element positioning in an array using 2 bases $(N_1 = 2, N_2 = 5)$ | 31 |
| 4. | Comparison of redundancy ratios for two bases | 32 |
| 5. | Element positions in a residue array formed using 3 bases $(N_1 = 2, N_2 = 3, N_3 = 4)$ | 33 |
| 6. | Comparison of redundancy ratios for three bases | 34 |
| 7. | Element positioning in an array using 3 bases $(N_1 = 2, N_2 = 2, N_3 = 3)$ | 35 |
| 8. | Comparison for example 1 | 36 |
| 9. | Element positioning in an array using 3 bases $(N_1 = 2, N_2 = 3, N_3 = 3)$ | 39 |
| 10. | Comparison for example 2 | 40 |
| 11. | Element positioning in an array using 3 bases $(N_1 = 2, N_2 = 3, N_3 = 4)$ | 43 |
| 12. | Comparison for example 3 | 44 |
| 13. | Element positioning in an array using 3 bases $(N_1 = 2, N_2 = 3, N_3 = 5)$ | 47 |
| 14. | Comparison for example 4 | 48 |
| 15. | Element positioning in an array using 3 bases $(N_1 = 3, N_2 = 3, N_3 = 4)$ | 52 |
| 16. | Comparison for example 5 | 53 |

ACKNOWLEDGMENT

In appreciation for their time, effort, and patience, many thanks go to my instructors, advisors, and fellow students. A special mention goes to my advisor, Professor David C. Jenn, thank you for your insight, extreme patience and precious goodwill. To Professor P. E. Pace, thank you for your direction and advice. I would also like to thank those who made this tour possible back home. But most of all, I would like to thank my friend and partner in life, my wife for her unselfish devotion and patience.

I. INTRODUCTION

The determination of the direction of an emitter of electromagnetic radiation is an important component of electronic warfare. Direction Finding (DF) information is usually provided by a listening antenna. If the direction of the antenna's main beam (or null) is known, then when the received power is a maximum (or minimum), the antenna is assumed pointed at the emitter. The search can be done either mechanically by physically turning the antenna, or electronically by comparing phased signals from two closely spaced elements.

Recently, electronic scanning has become the method of choice for high-performance DF systems. Array antennas can generally isolate emitters faster and more precisely. They also eliminate the need for moving parts, which is a serious problem for other types of large antennas. Large antennas are required for high resolution; that is, to separate two closely spaced emitters. Arrays also have the advantage of being flexible because they are electronically controlled. Some radiation pattern characteristics can be modified by simply reprogramming the beam controller. On the other hand, for a reflector antenna, such a modification would require a redesign of the feed antenna.

Conventional array antennas incorporate identical elements that are equally spaced. If N elements are uniformly distributed along a length L (referred to as the "array baseline"), the interelement spacing is $d = (N-1)/L$. In order to obtain a good input match for the elements and to avoid grating lobes, d is generally restricted to the range $0.25\lambda_0 \leq d \leq 0.75\lambda_0$ (where λ_0 is the wavelength).

If a linear array forms a conventional radiation beam, the beam width is approximately $0.88\lambda_0/L$ radians. Thus, to resolve two emitters that are separated by less than 1 degree apart can require an extremely large base line array. The attendant weight and beamforming network complexity can be reduced somewhat by thinning the array. Thinning can be done randomly (only practical when $N \gg 1$), or unequal spacings can be employed in the design of the array.

In principle, reducing the number of elements does not reduce the resolution as long as the baseline remains unchanged. However, the number of emitter directions that can be

determined simultaneously, denoted by M , depends on the number of elements. For the equally spaced N element array, $M = N - 1$. [1].

By making use of a theorem by Caratheodory [2], it can be shown that for a given number of elements, there exists a distribution of element positions which, for uncorrelated sources, results in superior spatial spectrum estimators than are otherwise achievable. In fact, Moffet [3] has examined the so-called optimum Minimum-Redundancy Array (MRA), for which integer numbers of d occur only once. Such an array can have a baseline much larger than $(N - 1)d$ and can potentially resolve as many as $M = N(N - 1)/2$ emitters. This is a dramatic increase over the number for the conventional equally spaced array.

The problem with the optimum MRA is twofold. First, the locations can only be determined by trial and error. For instance assume that our objective is to design an optimum MRA with N elements. In other words, disperse the N elements over a baseline, L with unequal spacings md , where m is an integer. Furthermore, all integers $1 \leq m \leq \frac{L}{d} - 1$ must occur once and only once, and none can be omitted. (This is denoted as the zero redundancy restricted case by Moffet). The solution is simply to search all possible element configurations and choose the one that satisfies the stated conditions. For a 10 element array with a baseline of $36d$, the number of possibilities is greater than 6×10^{10} [3]. Thus even with today's fast computers, finding the optimum MRA for large arrays is not practical.

A second problem with the optimum MRA is that the element locations are strictly defined. In some cases, it may not be possible to place an element at a prescribed location because of the platform (aircraft or ship) geometry or other structural limitations.

To circumvent the two problems described above, a new element placement procedure is investigated based on residue number systems (RNS). The element locations are obtained from simple modulo computations, and by varying the base of the number systems incorporated in the method, different configurations are generated. The residue array does not achieve the minimum redundancy of the optimum array, but has significantly lower redundancy than the conventional periodic array. In other words, some spacings may be repeated, while others are missing. The effect of these shortcomings on

the array response is shown to be relatively minor if the number of missing spacings is small compared to the total number.

In Chapter II array theory is reviewed with particular emphasis on the vector representation for antenna beamforming. Array performance is governed by its covariance matrix, and it is shown that the DF problem can be reduced to a matrix eigenvalue problem. The response of a conventional array is computed as an example and reference for subsequent comparisons.

Chapter III addresses the problem of element location selection. First, MRAs are introduced and the restricted and general cases defined. Next, the residue method is defined and data from several residue array configurations summarized in terms of a normalized redundancy ratio, R_n . This quantity is a measure of the redundancy of the residue array relative to the optimum MRA; thus $R_n = 1$ is ideal.

Chapter IV presents simulation data for a range of array parameters. Chapter V presents conclusions and recommendations for further research. Computer code listings are included in the Appendices.

II. ARRAY BEAMFORMING

A. INTRODUCTION

An array antenna is formed by combining the outputs (or inputs) of a collection of individual smaller radiation elements. In most cases, the elements of an array are identical. This is not necessary, but it is often convenient, simpler, and more practical. The individual elements of an array may be of any form (wires, apertures, etc.).

The total field of the array is determined by the vector addition of the fields radiated by the individual elements. To provide specialized radiation patterns, it is necessary that the fields from the elements of the array interfere constructively (add) in the desired signal directions and interfere destructively (cancel each other) in the direction of interferers. Ideally this can be accomplished, but practically it is only approached. In an array, there are five controls that can be used to shape the overall pattern of the antenna. These are:

1. the geometrical configuration of the overall array (linear, circular, rectangular, spherical. etc.),
2. the relative displacement between the elements,
3. the excitation amplitude of the individual elements,
4. the excitation phase of the individual elements, and
5. the relative pattern of the individual elements.

The simplest and one of the most practical arrays is formed by uniformly distributing the elements along a line. This arrangement is the conventional linear array configuration. If all of the array elements are identical, the principle of pattern multiplication applies [4]. It states that the total array pattern is given by the product of an element factor (EF) and an array factor (AF). Thus,

$$E(\theta, \phi) = EF(\theta, \phi) \cdot AF(\theta) \quad (2-1)$$

where $E(\theta, \phi)$ is the total radiated (or received) electric field intensity in the direction (θ, ϕ) . The array gain pattern is proportional to the magnitude square of the electric field pattern

$$G(\theta, \phi) \sim |E(\theta, \phi)|^2. \quad (2-2)$$

In subsequent discussions the element factor is suppressed by considering isotropic radiating elements. This simplification gives

$$G(\theta) \sim |AF(\theta)|^2. \quad (2-3)$$

B. ARRAY FACTOR FOR AN EQUALLY SPACED ARRAY

The array factor can be obtained by considering the elements to be point sources. Referring to Figure 1, if all elements are equally excited, the array factor is given by [4]

$$AF = w_0 + w_1 e^{j(kd \cos \theta + \beta)} + w_2 e^{j2(kd \cos \theta + \beta)} + \dots + w_{N-1} e^{j(N-1)(kd \cos \theta + \beta)}$$

$$AF = \sum_{n=1}^N w_{n-1} e^{j(n-1)(kd \cos \theta + \beta)} \quad (2-4)$$

which can be written as

$$AF = \sum_{n=1}^N w_{n-1} e^{j(n-1)\psi} \quad (2-5)$$

where $\psi = k_0 d \cos \theta + \beta$, $\beta = k_0 d \cos \theta_s$ (θ_s = beam scan angle), and $k_0 = 2\pi/\lambda_0$. For a uniformly excited array all of the coefficients in (2-5) are equal ($w_n = 1$, $n = 1, 2, \dots, N$). Thus, in this case, equation (2-5) can be written as

$$AF = \left[\frac{e^{jN\psi} - 1}{e^{j\psi} - 1} \right] = e^{j[(N-1)/2]\psi} \left[\frac{e^{jN/2\psi} - e^{-jN/2\psi}}{e^{j1/2\psi} - e^{-j1/2\psi}} \right] = e^{j[(N-1)/2]\psi} \left[\frac{\sin(\frac{N}{2}\psi)}{\sin(\frac{1}{2}\psi)} \right]. \quad (2-6)$$

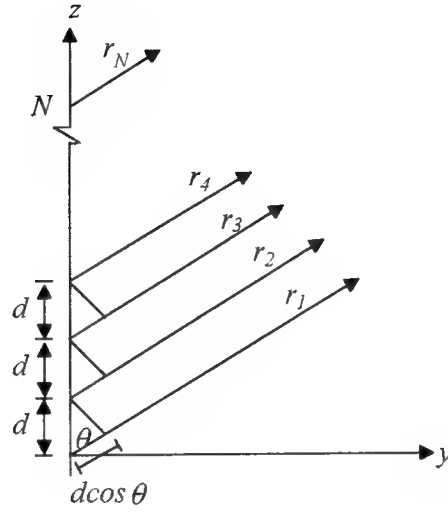


Figure 1. Far-field geometry of N -element array of isotropic sources positioned along the z -axis (From [4]).

If the phase reference point is the physical center of the array, the argument of the exponential is zero and the array factor reduces to

$$AF = \left[\frac{\sin(\frac{N}{2}\psi)}{\sin(\frac{1}{2}\psi)} \right] \quad (2-7)$$

The maximum value of the array factor is equal to N . To normalize the array factors so that the maximum value of each is equal to unity, equation (2-7) is divided by N

$$AF_{\text{norm}} = \frac{1}{N} \left[\frac{\sin(\frac{N}{2}\psi)}{\sin(\frac{1}{2}\psi)} \right] \quad (2-8)$$

The closed form result of equation (2-8) only occurs because the elements are equally excited. If the excitations vary from element to element, the coefficients of the exponentials in equation (2-4) are not equal.

C. DEGREES OF FREEDOM

Note that equation (2-4) is an N th degree polynomial with coefficients $\{w_n\}$. There are a total of $N-1$ degrees of freedom because there are $N-1$ coefficients that can be chosen independently. In a typical design scenario, one degree of freedom is used to point the main beam in the direction of the desired signal, leaving $N-2$ degrees of freedom to the null emitters [1]. The polynomial representation of array patterns has been used extensively to synthesize the radiation patterns by the placement of the nulls on the complex plane [5].

D. COVARIANCE MATRIX OF AN ARRAY

An array's response to multiple simultaneous sources can be determined using the representation shown in Figure 2. The complex weights $\{w_n\}$ are used to control the radiation pattern. A thinned array can be represented as an equally spaced array with the appropriate weights set to zero.

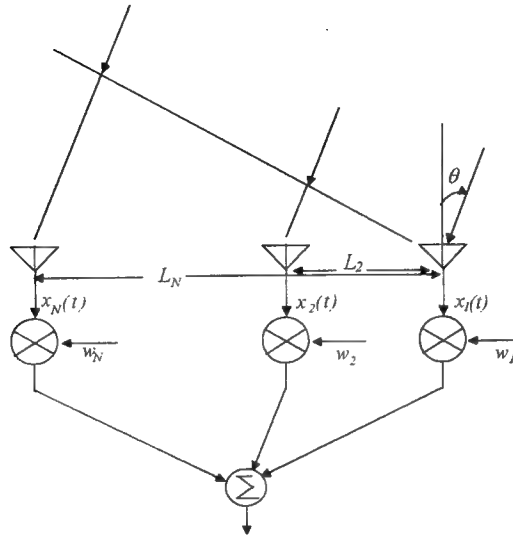


Figure 2. An N -element adaptive array.

The output of the n th element for a narrow-band signal, $s(t)$, in the direction θ at time t is

$$x_n(t) = s(t) e^{-jk_0 d_n \cos \theta} + n_n(t) \quad (2-9)$$

where d_n is the distance of element n from the phase reference (chosen to be at element 1). Thermal element noise is assumed present and denoted $n_n(t)$. It is zero mean and Gaussian distributed with variance $\sigma_n^2 = N_0$.

The array output response is obtained by summing the contributions from all elements

$$y(t) = \sum_{n=1}^N w_n x_n(t) \quad (2-10)$$

or, in vector notation, with T denoting transpose,¹

$$y(t) = W^T X(t) \quad (2-11)$$

where

$$W^T = [w_1 \ w_2 \ \dots \ w_N] \quad (2-12)$$

and

$$X(t) = \begin{bmatrix} x_1(t) \\ x_2(t) \\ \vdots \\ x_N(t) \end{bmatrix}. \quad (2-13)$$

The mean output power is obtained from the expected value of the output signal

$$E \{ |y(t)|^2 \} = E \{ y^*(t) y(t) \} = E \{ [W^T X(t)]^* [X(t) W^T] \} \quad (2-14)$$

$$= W^T E \{ X(t)^* X(t)^T \} W. \quad (2-15)$$

Now define the autocorrelation or covariance matrix as

$$R_{xx} = \{ X(t)^* X(t)^T \}. \quad (2-16)$$

The elements of the covariance matrix are given by

Vectors and matrices are denoted by capital letters.

$$[R_{xx}]_{ij} = E \{X_i(t)^* X_j(t)\}. \quad (2-17)$$

However, the noise is uncorrelated from element to element yielding

$$R_{xx} = R_{ss} + R_{nn}. \quad (2-18)$$

The signal autocorrelation matrix is

$$\begin{aligned} [R_{ss}]_{ij} &= E \{ (s(t) e^{-jk_0 d_i \cos \theta})^* (s(t) e^{-jk_0 d_j \cos \theta}) \} \\ &= P_s e^{jk_0 (d_i - d_j) \cos \theta} \end{aligned} \quad (2-19)$$

where $P_s = E \{ |s(t)|^2 \}$ is the signal power. The noise autocorrelation function is

$$[R_{nn}]_{ij} = E \{ n_i(t)^* n_j(t) \} = N_0 I. \quad (2-20)$$

where I is the identity matrix.

Up to this point the signal vector has only consisted of a single source. If K sources are present $s_k(t)$, $k = 1, 2, \dots, K$, with signal powers P_k , arriving from directions θ_k , then

$$x_i(t) = \sum_{k=1}^K s_k(t) e^{-jk_0 d_i \cos \theta_k} + n_i(t). \quad (2-21)$$

The corresponding covariance matrix has elements given by

$$[R_{xx}]_{ij} = \sum_{k=1}^K P_k e^{jk_0 (d_i - d_j) \cos \theta_k} + N_0 \delta_{ij} \quad (2-22)$$

where δ_{ij} is the Kronecker delta.

E. MATRIX DECOMPOSITION FOR DIRECTION OF ARRIVAL

In vector form equation (2-21) can be written as

$$X(t) = A^* S(t) + N(t) \quad (2-23)$$

where

$$N(t) = [n_1(t) \ n_2(t) \ \dots n_N(t)]^T, \quad (2-24)$$

$$S(t) = [s_1(t) \ s_2(t) \ \dots s_K(t)]^T. \quad (2-25)$$

The vector A contains the propagation delays

$$A = [U_1 \ U_2 \ \dots U_K] \quad (2-26)$$

where $U_k = U(\theta_k)$ and, for equally spaced elements,

$$U(\theta) = \begin{bmatrix} e^{jk_0 d_1 \cos \theta} \\ \vdots \\ e^{jk_0 d_N \cos \theta} \end{bmatrix} = \begin{bmatrix} 1 \\ e^{jk_0 d \cos \theta} \\ \vdots \\ e^{jk_0 (N-1)d \cos \theta} \end{bmatrix}. \quad (2-27)$$

Thus, the signal correlation matrix can now be written as

$$R_{xx} = A R_{ss} A' + N_0 I \quad (2-28)$$

where $'$ stands for the complex conjugate transpose, and I represents the identity matrix. For an equally spaced array with N elements located at $0, d, 2d, \dots, (N-1)d$ the size of the correlation matrix in equation (2-28) is $N \times N$. In this case, the maximum number of emitters that can be detected cannot exceed $(N-1)$.

The matrix R_{xx} is Hermitian and always positive definite if thermal element noise is present ($N_0 \neq 0$). Thus R_{xx} can be diagonalized using a rotation matrix E where

$$ER_{xx}E^t = \begin{bmatrix} \lambda_1 & & 0 \\ & \ddots & \\ 0 & & \lambda_N \end{bmatrix}. \quad (2-29)$$

The matrix E is unitary ($EE^t = I$) and its columns are the eigenvectors of R_{xx} , where

$$E = [e_1 \ e_2 \ \dots \ e_N]. \quad (2-30)$$

The signal covariance matrix is diagonalized by the same rotation matrix. For example, if there is only one signal present ($K = 1$) then

$$ER_{ss}E^t = \Lambda = \begin{bmatrix} \lambda & & 0 \\ & \ddots & \\ 0 & & 0 \end{bmatrix}. \quad (2-31)$$

In light of equation (2-15) the weight vector for the single signal case is

$$W = (\text{constant})e_1. \quad (2-32)$$

A measure of the array response is given by the spectral estimator

$$P(\theta) = \frac{1}{|H^*U(\theta)|^2} = \frac{1}{|e_1^t U(\theta)|^2}. \quad (2-33)$$

High values of P denote high array sensitivity; that is, a pattern notch or null at θ . Note that this is not the same condition that provides good signal-to-noise (high gain) for a conventional array. If more than one emitter is present the spectral estimator becomes

$$P(\theta) = \frac{1}{|[e_1 \dots e_{N-K}]^T U(\theta)|^2} . \quad (2-34)$$

The response for a conventional equally spaced array of 6 elements using ordinary beamforming is shown in Figure 3. In this case there is no ability to resolve two signals, the null locations are fixed relative to each other. Figure 4 shows the response of a Caratheodory array with four elements located at $0, d, 5d/2$, and $3d$. The emitter directions are at 35, 60, 90, 100, 125 and 150 degrees respectively. Note that all of the emitters are essentially resolved (i.e., peaks at the proper angles), but the sensitivity is only 10 dB in some cases.

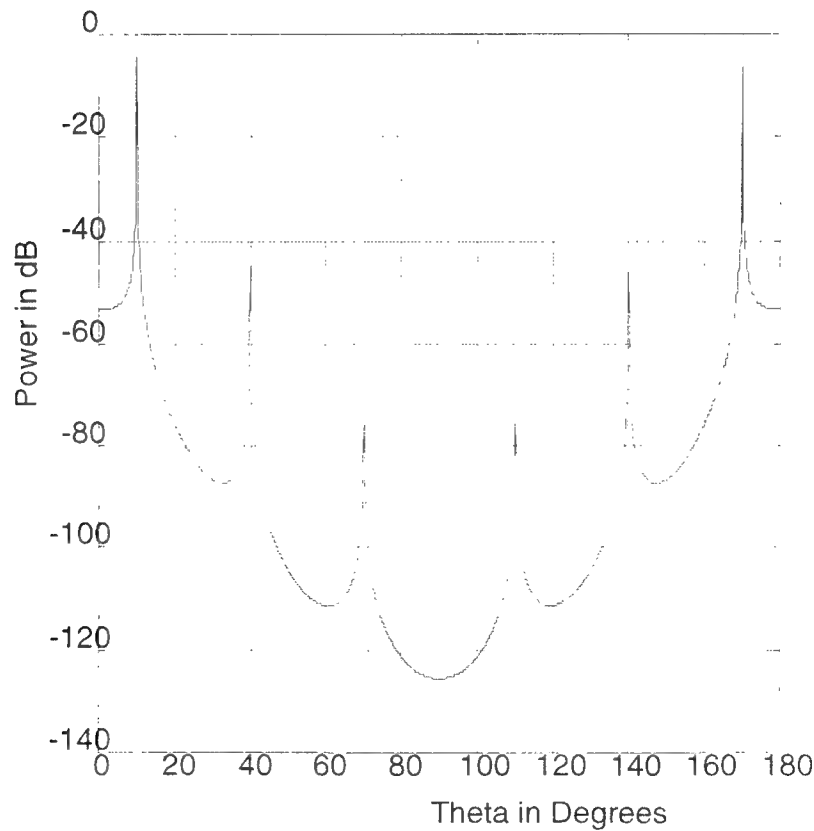


Figure 3. Conventional equally spaced array with $L = 6d$, $N = 6$.

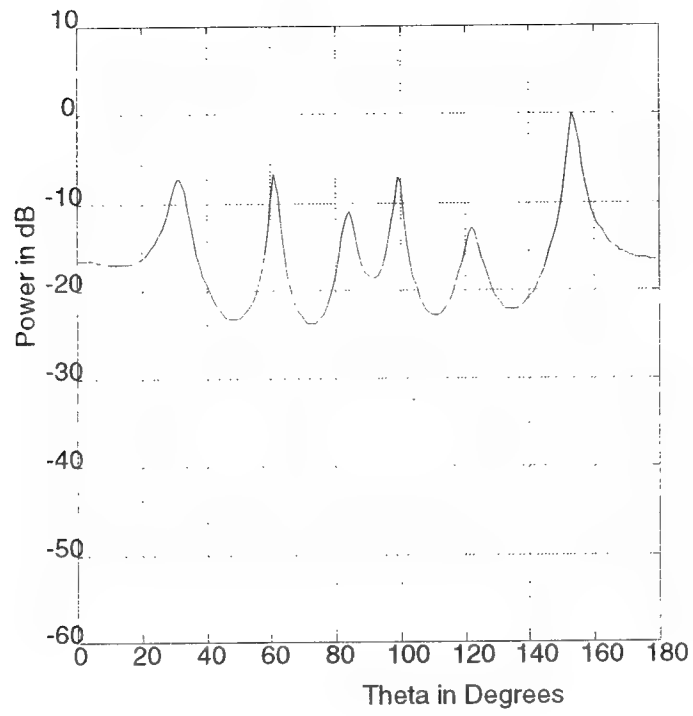


Figure 4. Conventional processing scheme for a C-array with $L = 6d$, $N = 4$.

F. METHODS FOR IMPROVED SPATIAL SPECTRUM ESTIMATION

Several processing methods exist to enhance the spectral estimation for multiple wave fronts. Two essentially equivalent techniques are the MUSIC method [6], and the theorem of Caratheodory (or C-arrays)[2]. They lead to asymptotically unbiased estimates of general signal parameters approaching the Cramer-Rao accuracy bound.

Caratheodory's theorem in the context of finite moment problems is of special significance. The most important property of the theorem is that, given a number of elements $M+1$ that satisfy $c_n^* = c_n$, there exists an integer K , $1 \leq K \leq M$, and certain constants $\alpha_k > 0$, and ω_k , for $k = 1, 2, \dots, K$, such that

$$c_m = \sum_{k=1}^K \alpha_k e^{-jm\omega_k} + \alpha_0 \delta_{ij}, \quad m = i - j = 0, 1, 2, \dots, M. \quad (2-35)$$

Furthermore, the integer K and the constants α_k and ω_k are determined uniquely. Comparing equation (2-22) and equation (2-35), it is clear that the autocorrelation lags represented by equation (2-22) have a Caratheodory representation as given in equation (2-35). Moreover, the similarity is exact if the N array element locations are spaced in such away that the set of integers (m) implied by the set of differences $(d_j - d_i) = m(d)$ ($i, j = 1, 2, \dots, N$) spans the integer set $(0, 1, \dots, M)$, where $N_{\max} = M \leq N(N-1)/2$. With N elements there are $(M+1)$ autocorrelation lags $r(m)$, where

$$r(m) = r(i - j) = \sum_{k=1}^K P_{sk} e^{jk_0 (d_i - d_j) \cos \theta_k} + N_0 \delta_{ij}, \quad m = 0, 1, 2, \dots, M. \quad (2-36)$$

The Caratheodory (C) sequence of length N defines the actual element location set $\{d_1, d_2, \dots, d_N\}$ which are integer multiples of a fundamental spacing d .

For the location of the directions of arrival, the autocorrelation matrix takes the form of a Toeplitz matrix

$$R_{xx} = \begin{bmatrix} r(0) & r(1) & \dots & r(M) \\ r^*(1) & r(0) & r(1) & \dots & r(M-1) \\ \vdots & \vdots & \ddots & \ddots & \vdots \\ r^*(M) & r^*(M-1) & \dots & \dots & r(0) \end{bmatrix} \quad (2-37)$$

where $r(m)$ is defined in equation (2-36). The matrix in (2-37) is called the augmented matrix, and is derived from the smaller matrix in equation (2-28). Using the matrix in equation (2-37) in a spatial spectrum algorithm, one can expect therefore to be able to handle a higher number of signal arrivals than could be handled using (2-28). This is shown explicitly for the specified case of a vector technique called MULTIPLE SIGNAL CLASSIFICATION (MUSIC) by Schmit[6].

From equation (2-22) and (2-28) $AR_{ss}A^t$ is of rank K and hence the lowest eigenvalue N_0 of R_{xx} has a multiplicity of $(M-K+1)$. By defining e_i as the corresponding eigenvectors where $i = K+1, K+2, \dots, M+1$

$$R_{xx}e_i = N_0 e_i. \quad (2-38)$$

Using (2-28), this gives $A^t e_i = 0$ which implies

$$U^t(\theta) e_i = 0 \quad (2-39)$$

for all $i = K+1, K+2, \dots, M+1$ and $k = 1, 2, \dots, K$. This implies further that the corresponding eigenvectors are orthogonal to signal direction vectors.

These noise eigenvectors can be used to form a spectral estimator $\tilde{P}(\theta)$ for the augmented matrix similar to (2-33) given by

$$\tilde{P}(\theta) = \frac{1}{\| [e_{K+1}, e_{K+2}, \dots, e_{M+1}]^t U(\theta) \|^2} \quad (2-40)$$

which can always be computed for $K \leq M$. Equation (2-40) implies that the maximum number of sources whose directions of arrival can be estimated using an augmented matrix is equal to N_{\max} . Here N_{\max} is the greatest multiple of the unit spacing d such that all multiples of the unit spacing $\leq N_{\max}$ are present between pairs of elements array. In this case $N_{\max} > N$ and may be as high as $N(N-1)/2$.

Figure 5 shows the spectrum of the C-array considered in Figure 4 obtained using the augmented matrix. It is apparent from a comparison of Figures 4 and 5 that there is an improvement in dynamic range (the signal peaks to the background level) relative to ordinary beamforming.

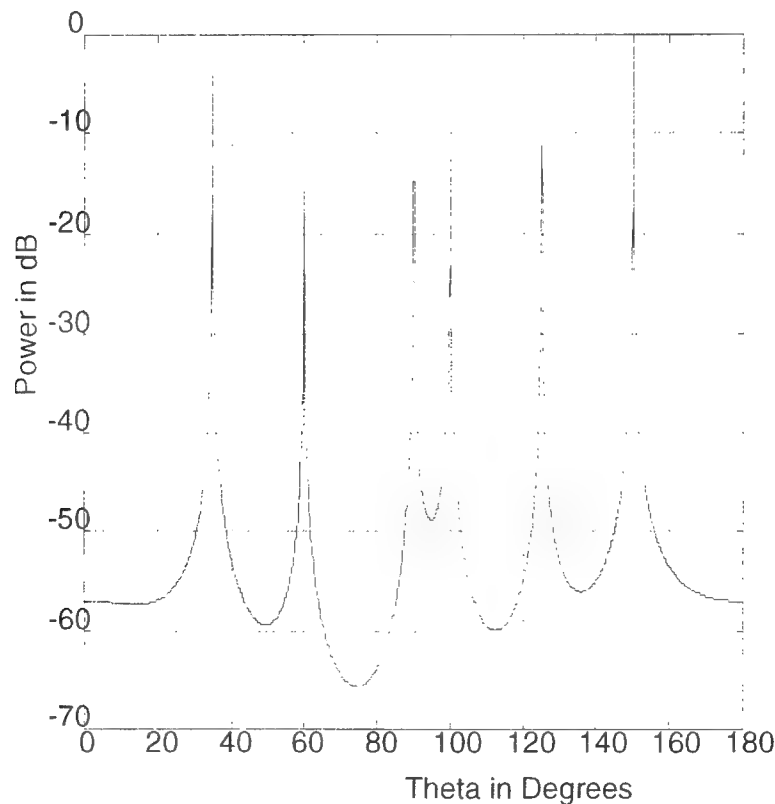


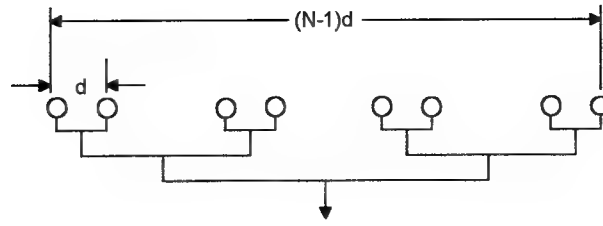
Figure 5. The improved spatial spectrum estimation using the augmented matrix for a C-array with $L = 6d$ and $N = 4$.

III. MINIMUM-REDUNDANCY LINEAR ARRAYS

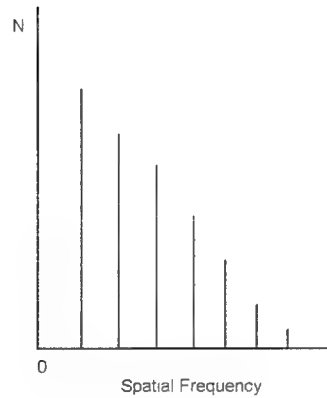
A. INTRODUCTION

As mentioned in the previous chapter, the linear array is one of the most important types of direction finding antennas. Existing work on the design of linear arrays has mainly been concerned with the problems of feeding many elements and with tapering the illumination of the aperture to obtain a desired beam shape or degree of sidelobe suppression. However, in arrays designed for the resolution of closely-spaced sources, the paramount requirement is to maximize the aperture dimensions and collecting area for a given number of elements.

Moffet [3] has investigated the use of linear arrays in radio astronomy for observations of the sun. A diagram of a typical grating array (i.e., periodic array) is shown in Figure 6(a). Equal-length branching transmission lines are used to combine the signals from the individual elements at a single receiver input. The spatial-frequency sensitivity diagram for the array is shown in Figure 6(b). Clearly there is a very high degree of redundancy present. In an N -element grating, the unit spacing (d) is present $N-1$ times, twice-unit spacing ($2d$) is present $N-2$ times, and so forth out to the maximum spacing of $(N-1)d$, which is present just once. Higher resolution can be achieved for a given N if the number of redundant spacings were reduced, permitting the length of the array to be increased.



(a)



(b)

Figure 6. (a) Grating interferometer with $N=8$. (b) Spatial sensitivity diagram for the grating interferometer.

The high degree of redundancy in the periodic array permits the simple feeder arrangement shown in Figure 6(a). The antenna pattern has the form $[\sin(NX)/(N \sin X)]^2$ and the number of distinct emitters which can be resolved in a one-dimensional source distribution is approximately equal to N . This is obtained when the angular width of the emitters are equal to the separation between the lobes. The unit spacing d determines the size of the field over which the array produces an unambiguous picture of the source distribution.

B. OPTIMUM MINIMUM-REDUNDANCY ARRAYS

The minimum-redundancy array was considered by Arsac [7] who constructed the largest possible linear arrays for a given N having zero redundancy. There are four such arrays shown in Figure 7. The first is the trivial case of a single-element. In the others there is one, and only one, pair of elements separated by each multiple of the unit spacing out to a maximum spacing equal to the distance between the end elements. Thus each of these arrays uniformly samples the spatial-frequency spectrum out to a baseline spacing

$$L = \frac{1}{2}N(N-1)d = N_{\max}d \quad (3-1)$$

where $\frac{1}{2}N(N-1)$ is the number of possible pairs of N distinct elements. Bracewell [8] has given an elegant proof of uniqueness; that is, these are the only linear arrays having zero redundancy for the specified N .

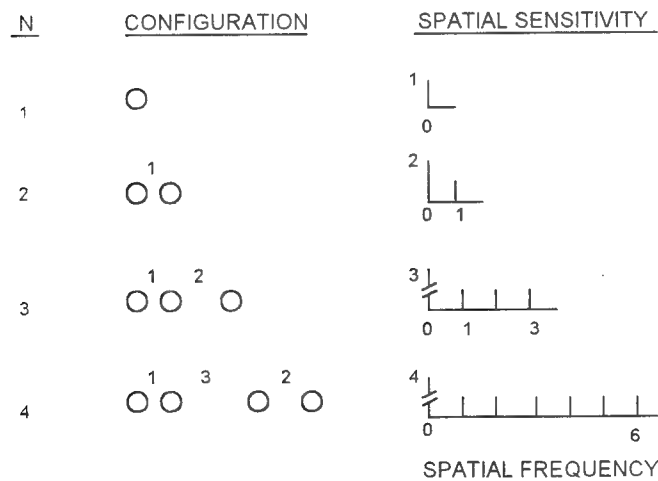


Figure 7. The four lowest N zero-redundancy linear arrays and their spatial sensitivity diagrams (From [7]).

It can be seen from Figure 7 that the zero-redundancy arrays sample the spatial-frequency spectrum at uniform intervals and with uniform sensitivity except for the zero spacing, or total power, component. The gain pattern which results has approximately the form $[\sin(NX)/(N\sin X)]$, and gives the highest possible resolution for a given aperture length. The result of scanning a source distribution with such a pattern is to reject all spatial components in the source with spatial frequency greater than the maximum to which the array is sensitive, yielding an image of the source known as the principal solution. It is not necessary that the array sample the spatial-frequency spectrum of the source at exactly uniform intervals, but the grating sidelobes will become serious at a distance from the main lobe equal to the inverse of the maximum spacing between samples (measured in wavelengths). Processing of the data from an array is very much simplified if the sampling is done at uniform intervals.

In an array with more than four elements, it is clear that there must be some configuration of the elements which leads to minimum redundancy while still retaining coverage of the spatial-frequency spectrum. A firm upper limit for the minimum redundancy is set by the rather simple division of the elements of the array into two equal groups, shown schematically in Figure 8(a) for the case $N = 8$. This is the compound grating interferometer [9]. With the branching feeder arrangement shown in Figure 8(a), the receiver sees the correlated signal between the narrow-spaced half of the elements and the wide-spaced half, giving uniform coverage of the spatial-frequency spectrum out to $(N^2/4)d$ (for even values of N). By accepting a more complex receiving arrangement in which the signals from the antennas are individually correlated with each other, the spacing between elements in the wide-spaced half may be increased to $(N/2 + 1)d$, giving coverage out to $(N^2/4 + N/2 - 1)d$. This arrangement is shown in Figure 8(b).

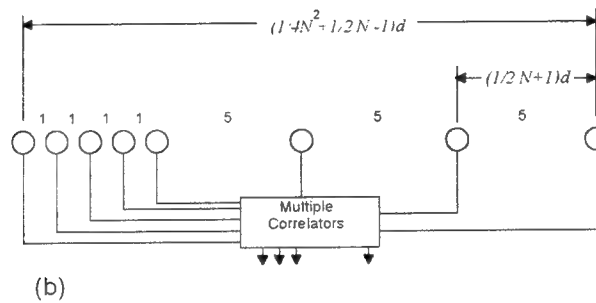
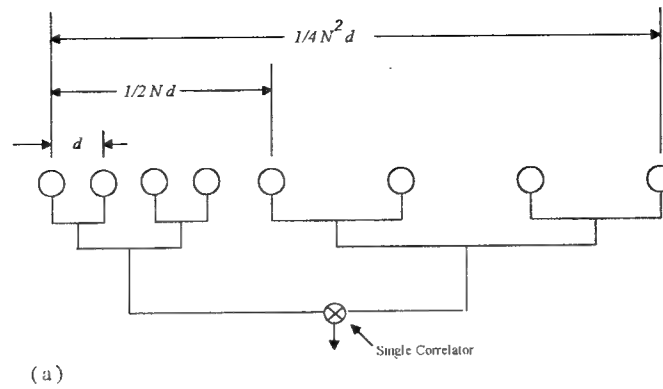


Figure 8. (a) Compound grating interferometer with branching feeds and a single correlation detector. (b) Modified compound grating interferometer.

The redundancy factor R_r may be defined by the ratio of the number of pairs to N_{\max} , i.e.,

$$R_r = \frac{\frac{1}{2}N(N-1)}{N_{\max}}. \quad (3-2)$$

For large values of N , the redundancy approaches $N^2/(2 N_{\max})$. The configuration in Figure 8(a) has a redundancy of 1.75 ($0.5 \times 8 \times 7/16$) and that in Figure 8(b) a redundancy of 1.47 ($0.5 \times 8 \times 7/19$). The $16d$ and $19d$ are the length of each compound grating respectively.

The arrangement in Figure 8(b) has appreciable advantage only for limited values of N ; for large values of N , the aperture width tends toward $\frac{1}{4}N^2d$ for either arrangement. Since the number of distinct pairs $N(N-1)/2$ tends toward $N^2/2$, the redundancy factor in these compound grating arrays is always ≤ 2 .

A plot of the redundancy R_r as a function of N for a fixed length L shows that the redundancy decreases with N until it reaches a certain minimum value referred to as the minimum redundancy. Beyond this point the redundancy goes up. An example of this is shown in Figure 9 where the length of the array is kept constant at $L = 19d$ and the number of elements is varied from $N= 2$ to 19. The lowest value of R_r was found to be 1.1538 at $N = 6$.

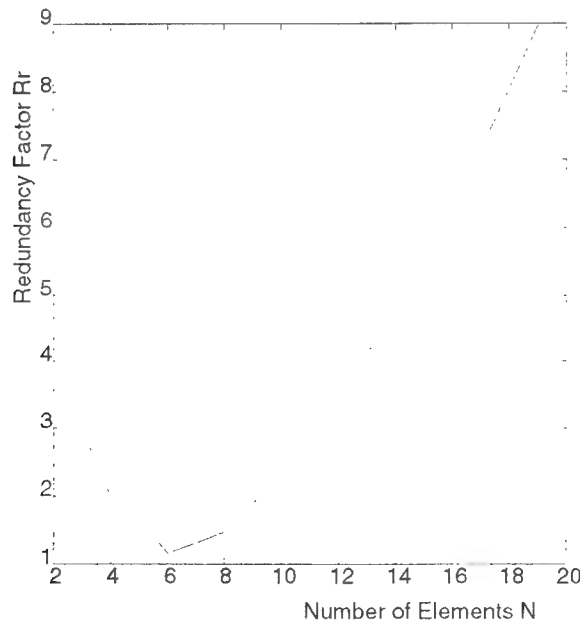


Figure 9. The redundancy R_r vs the number of elements N with the length fixed at $L = 19d$.

Finding the array configuration giving the lowest possible redundancy for a given number of elements is not a trivial matter. Leech [10] has examined this identical problem in the theory of numbers, and gives some solutions for $N \leq 11$. He demonstrated that in the limit of large N , the minimum redundancy lies between 1.217 and 1.332.

1. Restricted Case vs General Case

There are two categories of MRAs: (1) the restricted case and, (2) the general case. In the restricted case, the whole distance of the array (L) is uniformly covered. This means that the spatial frequency spectrum is uniformly covered up to a spacing $N_{\max}d$, i.e. the distance between the end elements of the array. An example of this case is shown in Figure 10. In this case the configurations 1-1-9-4-3-3-2 and 1-3-6-6-2-3-2 all have $N_{\max}d$ equal to the actual length of the array L which is $23d$.

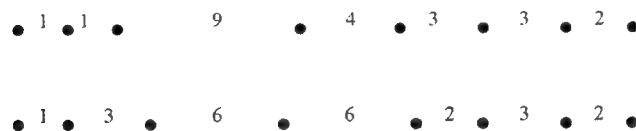


Figure 10. The two restricted minimum-redundancy eight-element arrays.

In the general case, the actual length of the array can be greater than $N_{\max}d$. The remaining spacings, which number $\frac{1}{2}N(N-1) - N_{\max}$ are not all redundant since some exceed $N_{\max}d$. In this case, the coverage of the spatial-frequency spectrum is uniform only up to $N_{\max}d$. An example of this is shown in Figure 11. The configuration 8-10-1-3-2-7-8 has a total length of $39d$ with a redundancy of 1.17, while the value of N_{\max} is only 24.



Figure 11. The general minimum-redundancy eight-element arrays.

The additional resolution afforded by the larger overall length of the general array might be welcome, even though the spatial-frequency coverage is incomplete above $N_{\max}d$, providing enough space is available. In other applications, where there is not as much space to provide the extra length, the restricted array will be more attractive. Table 1 gives examples of restricted and general array configurations for $N = 5$ to 11.

Restricted Array

| N | N_{\max} | R | Configuration |
|-----|------------|------|---|
| 5 | 9 | 1.11 | - 1 - 3 - 3 - 2 - |
| 6 | 13 | 1.16 | - 1 - 5 - 3 - 2 - 2 - |
| 7 | 17 | 1.24 | - 1 - 3 - 6 - 2 - 3 - 2 - |
| 8 | 23 | 1.22 | - 1 - 3 - 6 - 6 - 2 - 3 - 2 - |
| 9 | 29 | 1.24 | - 1 - 3 - 6 - 6 - 6 - 2 - 3 - 2 - |
| 10 | 36 | 1.25 | - 1 - 2 - 3 - 7 - 7 - 7 - 4 - 4 - 1 - |
| 11 | 43 | 1.3 | - 1 - 2 - 3 - 7 - 7 - 7 - 7 - 4 - 4 - 1 - |

General Array

| N | N_{\max} | R | Configuration |
|-----|------------|------|--|
| 5 | 9 | 1.11 | - 4 - 1 - 2 - 6 - |
| 6 | 13 | 1.16 | - 6 - 1 - 2 - 2 - 8 - |
| 7 | 18 | 1.17 | - 14 - 1 - 3 - 6 - 2 - 5 - |
| 8 | 24 | 1.17 | - 8 - 10 - 1 - 3 - 2 - 7 - 8 - |
| 10 | 37 | 1.22 | - 16 - 1 - 11 - 8 - 6 - 4 - 3 - 2 - 22 - |
| 11 | 45 | 1.24 | - 18 - 1 - 3 - 9 - 11 - 6 - 8 - 2 - 5 - 28 - |

Table 1. Some minimum-redundancy array configurations (After [3])

2. Advantage and Disadvantage of MRA's

Looking at Figures 6, 10 and 11 it is possible to compare the eight-element arrays so as to deduce the advantages and disadvantages of each. One obvious advantage with the MRA of Figures 10 and 11 is that it gives more than three times the coverage of the spatial-frequency spectrum for equal values of unit spacing d , i.e., for equal grating lobe separations. The price for this greater coverage is a more complicated signal processing system and higher sidelobes. This can be overcome by the adjusting the correlator outputs. This is an easy modification for an array with digital beamforming. Using a digital computer, the beam can be tailored to have any desired sidelobe level by choosing appropriate weighting of the various correlator outputs representing different element separations. Another advantage of this system is that in the computer the electrical path lengths from each antenna to the correlators may be determined after the fact and corrections may be applied for any changes in these lengths. This eliminates the tedious adjustment of the feed lines in a grating array in which the signals from each antenna must be added together in exactly the right phase before detection.

A disadvantage of the minimum-redundancy array is that its resolution is not easily increased except by adding more elements and rearranging the array to the optimum configuration for the new number of elements. With the compound grating arrays, increased resolution is readily obtained by combining observations with different array configurations. For instance, the resolution of the array in Figure 8(a) may be doubled by taking an additional observation with the separation between the narrow-spaced and wide-spaced halves of the array increased by an amount equal to the length of the original array, $\frac{1}{4}N^2 d$. The two observations are combined coherently to achieve double the original resolution with the same grating lobe spacing.

It has already been mentioned that it is not an easy matter to work out the minimum-redundancy configuration for a large value of N . Leech [10] described several short cuts. A "brute force" search for the optimum ten-element array with $N_{\max}=36$ would

present approximately 6×10^{10} number of possible configurations even in the restricted case.

C. THE RESIDUE NUMBER SYSTEM (RNS)

1. Introduction

The ancient study of the *residue numbering system*, or RNS, begins with a verse from a third-century book, Suan-ching, by Sun Tzu [11] :

We have things of which we do not know the number,
If we count them by threes, the remainder is 2,
If we count them by fives, the remainder is 3,
If we count them by sevens, the remainder is 2,
How many things are there?
The answer, 23.

This 1700-year-old number system has been attracting a great deal of attention recently. Digital systems structured into residue arithmetic units may play an important role in ultra-speed, dedicated, real-time systems that support pure parallel processing of integer-valued data. It is a "carry free" system that performs addition, subtraction, and multiplication as concurrent (parallel) operations, side-stepping one of the principal arithmetic delays: managing carry information.

There are many applications that attempt to exploit the unique RNS properties. They include the study of error codes, the building of a special-purpose digital correlator and designing a general-purpose computing machine among others. Experimentally, these early efforts met with little success because winding the custom core memory required specialized residue mappings. The technology of the 60's was insufficient to support the unique demands of the RNS.

Since the mid-70's the situation has changed; technology and theory have been slowly converging. In the west, over 100 major papers have been published on RNS. In

addition, scholars in the former Soviet Union are actively investigated residue arithmetic. In this particular application residue arithmetic itself is not used, but the low redundancy patterns obtained by "overlaying" several RNSs are used to place array elements.

2. RNS Encoding For Arrays

The RNS is defined in terms of a set of pairwise relatively prime moduli. If N denotes the moduli set, then

$$N = \{N_1, N_2, \dots, N_L\}, \text{ GCD}(N_i, N_j) = 1, \text{ for } i \neq j \quad (3-3)$$

where GCD denotes the greatest common divisor. Any integer in the residue class Z_L , where Z_L is the ring of integers in modulo L , $[0, 1, \dots, L-1]$

and

$$L = N_1 \times N_2 \times \dots \times N_L \quad (3-4)$$

has a unique L -tuple representation given by

$$X \text{ RNS} \rightarrow (X_1, X_2, \dots, X_L) \quad (3-5)$$

where $X_i = X \bmod M_i$ and M_i is the base integer, is called the i th residue of X .

An example that illustrates the representation of a number X in a RNS is shown in Table 2. From Table 2:

$$3 \text{ RNS} \rightarrow (0, 3, 3)$$

$$7 \text{ RNS} \rightarrow (1, 3, 2)$$

$$11 \text{ RNS} \rightarrow (1, 2, 0)$$

$$60 \text{ RNS} \rightarrow (0, 0, 0)$$

| X | $N_1=3$ | $N_2=4$ | $N_3=5$ |
|----------|----------|----------|----------|
| 0 | 0 | 0 | 0 |
| 1 | 1 | 1 | 1 |
| 2 | 2 | 2 | 2 |
| 3 | 0 | 3 | 3 |
| 4 | 1 | 0 | 4 |
| 5 | 2 | 1 | 0 |
| 6 | 0 | 2 | 1 |
| 7 | 1 | 3 | 2 |
| 8 | 2 | 0 | 3 |
| \vdots | \vdots | \vdots | \vdots |
| 58 | 1 | 2 | 3 |
| 59 | 2 | 3 | 4 |
| 60 | 0 | 0 | 0 |

Table 2. An example to illustrate the encoding procedure for
 $(N_1 = 3, N_2 = 4, N_3 = 5)$.

3. Incorporation of RNS into Array design

This thesis examines the possibility of using RNS patterns to generate low redundancy arrays and to compare their performance to the optimal minimum redundancy array. The method of element placement is based on superimposing the locations of several arrays of different base lengths. For instance, bases 2 and 5 give element locations indicated by "0" in Table 3. Each row in Table 3 represents an increment of d . Thus, the prescribed element placements are $0d, 2d, 4d, 5d, 6d, 8d, 10d$. The length of the array is $L = (N_1 \times N_2)d = (2 \times 5)d = 10d$ and the number of elements is $N = 7$.

| Location | $N_1=2$ | $N_2=5$ | Element Position |
|----------|---------|---------|------------------|
| $0d$ | 0 | 0 | * |
| $1d$ | 1 | 1 | |
| $2d$ | 0 | 2 | * |
| $3d$ | 1 | 3 | |
| $4d$ | 0 | 4 | * |
| $5d$ | 1 | 0 | * |
| $6d$ | 0 | 1 | * |
| $7d$ | 1 | 2 | |
| $8d$ | 0 | 3 | * |
| $9d$ | 1 | 4 | |
| $10d$ | 0 | 0 | * |

Table 3. Element positioning in an array using 2 bases ($N_1=2, N_2=5$).

Using the above element placements the redundancy ratio (R_r) and the maximum number of received emitters (N_{\max}) can be found. They are compared to the periodic array and the optimum minimum redundancy array in Table 4. The normalized redundancy ratio R_n is the ratio of the redundancy factor of the array to that of the periodic array ($R_p = N/2$). It can be seen that the optimum MRA has lower redundancy than both the RNS and the periodic arrays. However, this is for a relatively small number of elements and a small array length. Moreover, the computation time to search the optimum configuration in this example is not a factor because of the small number of elements. For large numbers of elements certain combinations of bases yield redundancies closer to the optimum, and the processing time is much faster than that for the optimum.

| Array Type | R_r | N_{\max} | $R_n = R_r/R_p$ |
|----------------|-------|------------|-----------------|
| RNS | 3.5 | 6 | 0.78 |
| Optimum MRA | 2.1 | 10 | 0.47 |
| Periodic Array | 4.5 | 10 | 1 |

Table 4. Comparison of redundancy ratios for two bases.

The procedure can be extended to three bases as shown in Table 5. The prescribed element locations are $0d, 2d, 3d, 4d, 6d, 8d, 9d, 10d, 12d, 14d, 15d, 16d, 18d, 20d, 21d, 22d, 24d$. The length of the array is $L = (N_1 \times N_2 \times N_3)d = (2 \times 3 \times 4)d = 24d$ and the number of elements is $N = 17$. Once again, using the above element placements, the redundancy ratio (R_r) and the maximum number of received emitters (N_{\max}) can be found and compared to the periodic array and the optimum minimum redundancy array. The results are shown in Table 6.

| Location | $N_1=2$ | $N_2=3$ | $N_3=4$ | Element Position |
|----------|---------|---------|---------|------------------|
| $0d$ | 0 | 0 | 0 | * |
| $1d$ | 1 | 1 | 1 | |
| $2d$ | 0 | 2 | 2 | * |
| $3d$ | 1 | 0 | 3 | * |
| $4d$ | 0 | 1 | 0 | * |
| $5d$ | 1 | 2 | 1 | |
| $6d$ | 0 | 0 | 2 | * |
| $7d$ | 1 | 1 | 3 | |
| $8d$ | 0 | 2 | 0 | * |
| $9d$ | 1 | 0 | 1 | * |
| $10d$ | 0 | 1 | 2 | * |
| $11d$ | 1 | 2 | 3 | |
| $12d$ | 0 | 0 | 0 | * |
| $13d$ | 1 | 1 | 1 | |
| $14d$ | 0 | 2 | 2 | * |
| $15d$ | 1 | 0 | 3 | * |
| $16d$ | 0 | 1 | 0 | * |
| $17d$ | 1 | 2 | 1 | |
| $18d$ | 0 | 0 | 2 | * |
| $19d$ | 1 | 1 | 3 | |
| $20d$ | 0 | 2 | 0 | * |
| $21d$ | 1 | 0 | 1 | * |
| $22d$ | 0 | 1 | 2 | * |
| $23d$ | 1 | 2 | 3 | |
| $24d$ | 0 | 0 | 0 | * |

Table 5. Element positions in a residue array formed using 3 bases
($N_1 = 2, N_2 = 3, N_3 = 4$).

| Array Type | R_r | N_{\max} | $R_n = R_r/R_p$ |
|----------------|-------|------------|-----------------|
| RNS | 6.18 | 24 | 0.54 |
| Optimum MRA | 5.67 | 24 | 0.49 |
| Periodic Array | 11.5 | 24 | 1 |

Table 6. Comparison of redundancy ratios for three bases.

The results in Table 6 show an improvement in the redundancy of the RNS array to that of the optimum for a relatively high number of elements and long baselines. However, an inspection of the element positions (last column in Table 5) shows the repetition of a fundamental pattern. This is due to the fact that the spacing dictated by each base has a period, and therefore, when all are superimposed, the total configuration will have a period. The repetition is more noticeable in the example of Table 5 because one base ($N_3 = 4$) is the integer multiple of another ($N_1 = 2$).

IV. SIMULATION RESULTS

A. DATA

The effectiveness of the RNS approach to generating array configurations is evaluated for several examples. The redundancy factor (R_r) and the number of the received emitters N_{\max} for the RNS method are compared to those of the optimum method. Also, the antenna responses for both methods are plotted and compared. In this chapter the length will simply be denoted by the integer multiple of d .

Example 1:

The number of elements is $N=9$ and the length of the array $L=12$. Table 7 shows the three bases and element locations. Table 8 shows a comparison of the redundancy and the number of received emitters for the RNS and the optimum methods.

| Location | $N_1 = 2$ | $N_2 = 2$ | $N_3 = 3$ | Element Position |
|----------|-----------|-----------|-----------|------------------|
| $0d$ | 0 | 0 | 0 | * |
| $1d$ | 1 | 1 | 1 | |
| $2d$ | 0 | 0 | 2 | * |
| $3d$ | 1 | 1 | 0 | * |
| $4d$ | 0 | 0 | 1 | * |
| $5d$ | 1 | 1 | 2 | |
| $6d$ | 0 | 0 | 0 | * |
| $7d$ | 1 | 1 | 1 | |
| $8d$ | 0 | 0 | 2 | * |
| $9d$ | 1 | 1 | 0 | * |
| $10d$ | 0 | 0 | 1 | * |
| $11d$ | 1 | 1 | 2 | |
| $12d$ | 0 | 0 | 0 | * |

Table 7. Element positioning in an array using 3 bases
($N_1 = 2, N_2 = 2, N_3 = 3$).

| Array Type | R_r | N_{\max} |
|-------------|-------|------------|
| RNS | 3.6 | 10 |
| Optimum MRA | 3 | 12 |

Table 8. Comparison for example 1.

The antenna responses for the RNS and optimum cases are as shown in Figure 12 and Figure 13 respectively. For the optimum case $N_{\max} = 12$ and the emitter directions are 20, 35, 50, 60, 70, 80, 100, 110, 120, 130, 145, and 165 degrees. For the RNS array $N_{\max} = 10$ and the emitter directions are the same as those for the optimum. In this case the array response directions differ from the actual emitter directions because the matrix is overdetermined (number of emitters $> N_{\max}$). If two emitters are removed, the response directions are exactly the same as the emitter directions as shown in Figure 14. In this case the emitter directions are 30, 45, 60, 70, 80, 100, 110, 130, 140, and 160 degrees.

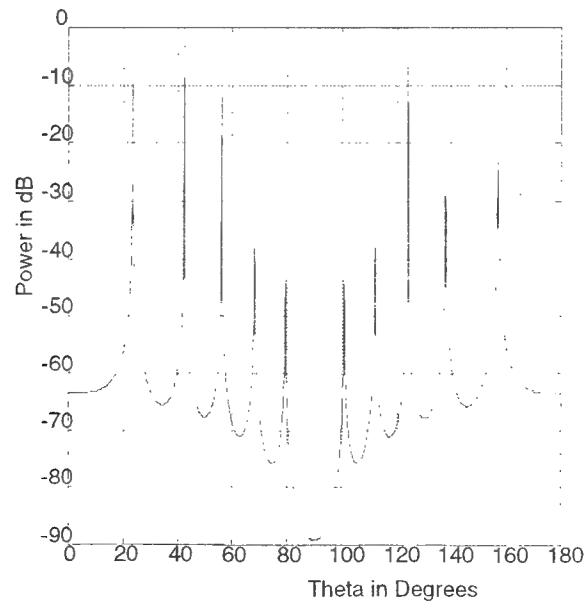


Figure 12. The RNS antenna response for $N = 9$, $L = 12$.

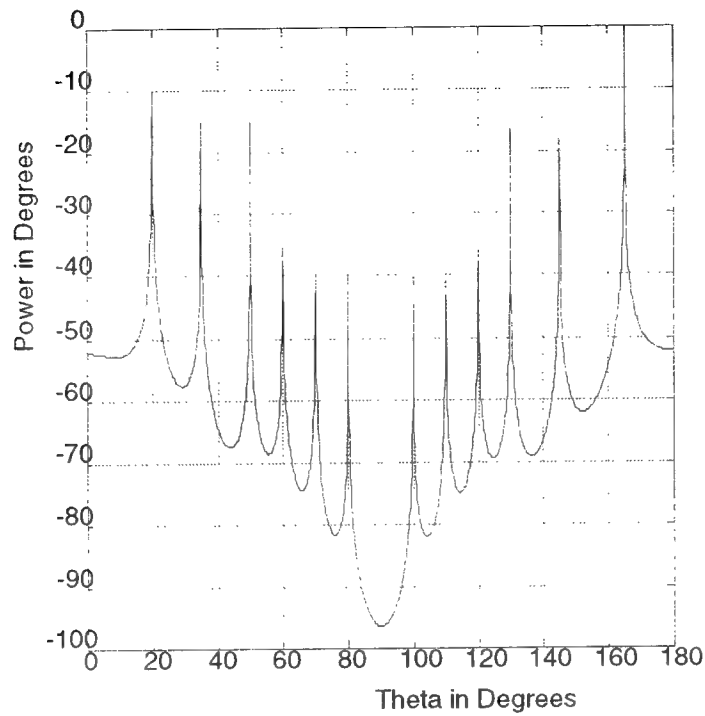


Figure 13. The optimum antenna response for $N = 9$, $L = 12$.

The results of Table 8, Figure 12 and Figure 13 indicate that the redundancy and the number of the received emitters are slightly better in the optimum array than for the RNS array for this particular set of emitters.

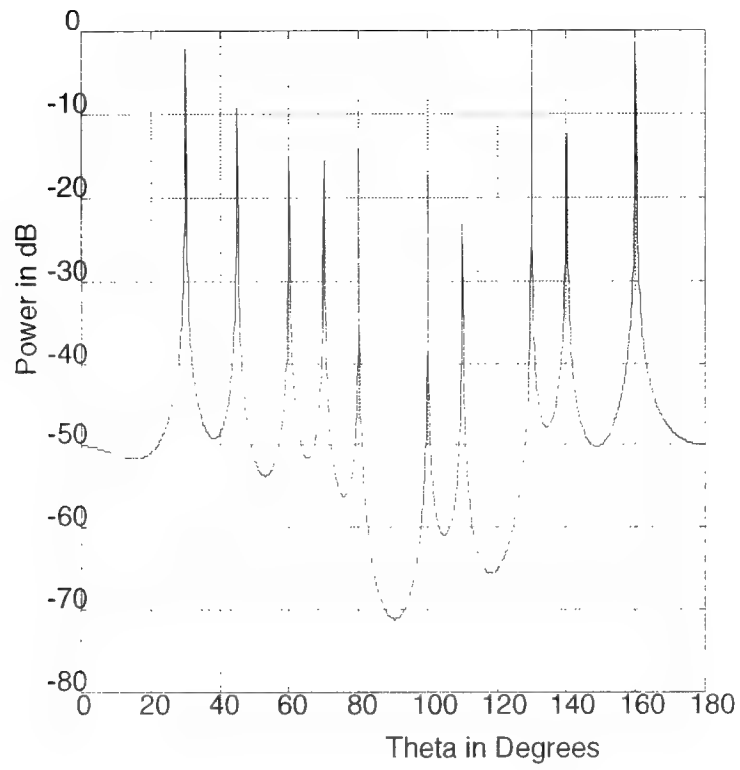


Figure 14. The RNS antenna response for $N=9$, $L=12$ and $N_{\max}=10$.

Example 2:

The number of elements is $N = 13$ and the length of the array $L = 18$. Note that this is just an extension of the array in Example 1. Table 9 shows the three bases and the element locations. Table 10 compares of the redundancy ratio and the number of received emitters for the RNS and the optimum arrays.

| Location | $N_1 = 2$ | $N_2 = 3$ | $N_3 = 3$ | Element Position |
|----------|-----------|-----------|-----------|------------------|
| $0d$ | 0 | 0 | 0 | * |
| $1d$ | 1 | 1 | 1 | |
| $2d$ | 0 | 2 | 2 | * |
| $3d$ | 1 | 0 | 0 | * |
| $4d$ | 0 | 1 | 1 | * |
| $5d$ | 1 | 2 | 2 | |
| $6d$ | 0 | 0 | 0 | * |
| $7d$ | 1 | 1 | 1 | |
| $8d$ | 0 | 2 | 2 | * |
| $9d$ | 1 | 0 | 0 | * |
| $10d$ | 0 | 1 | 1 | * |
| $11d$ | 1 | 2 | 2 | |
| $12d$ | 0 | 0 | 0 | * |
| $13d$ | 1 | 1 | 1 | |
| $14d$ | 0 | 2 | 2 | * |
| $15d$ | 1 | 0 | 0 | * |
| $16d$ | 0 | 1 | 1 | * |
| $17d$ | 1 | 2 | 2 | |
| $18d$ | 0 | 0 | 0 | * |

Table 9. Element positioning in an array using 3 bases
($N_1 = 2, N_2 = 3, N_3 = 3$).

| Array Type | R_r | N_{\max} |
|-------------|-------|------------|
| RNS | 4.88 | 16 |
| Optimum MRA | 4.33 | 18 |

Table 10. Comparison for example 2.

The antenna responses for the RNS and optimum cases are as shown in Figure 15 and Figure 16, respectively, for 18 emitters. The emitter directions are 10, 30, 40, 50, 55, 60, 70, 75, 80, 100, 105, 110, 115, 125, 130, 140, 150 and 170 degrees.

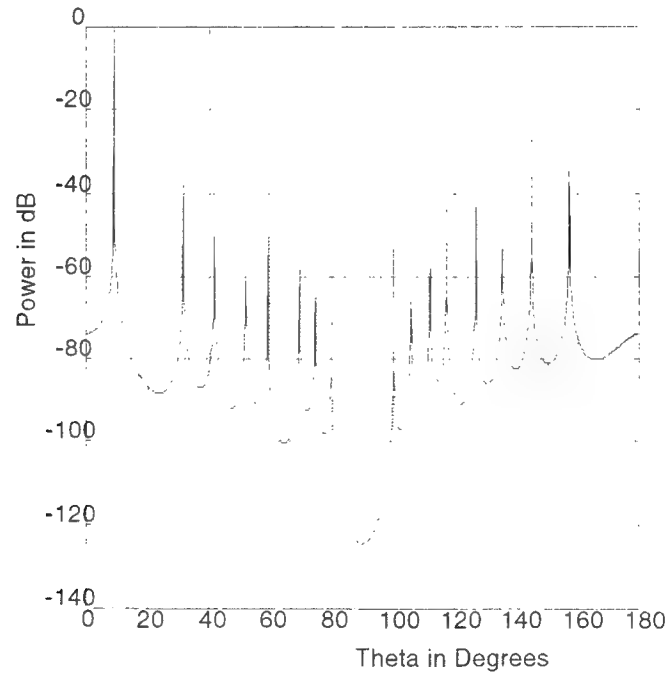


Figure 15. The RNS antenna response for $N = 13$, $L = 18$.

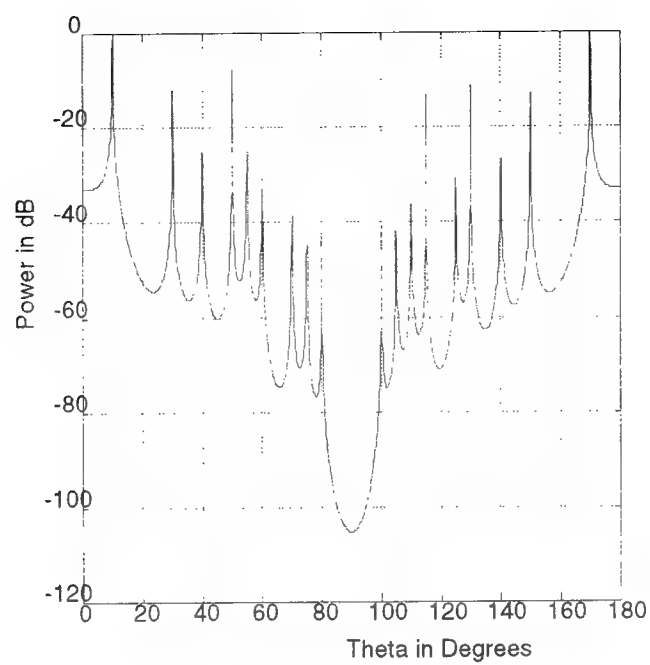


Figure 16. The optimum antenna response for $N = 13$, $L = 18$.

Figure 17 is a plot of the RNS antenna response for its maximum number of received emitters $N_{\max} = 16$. The new emitter directions are 10, 30, 40, 50, 60, 70, 75, 80, 100, 105, 110, 120, 130, 140, 150, and 160 degrees.

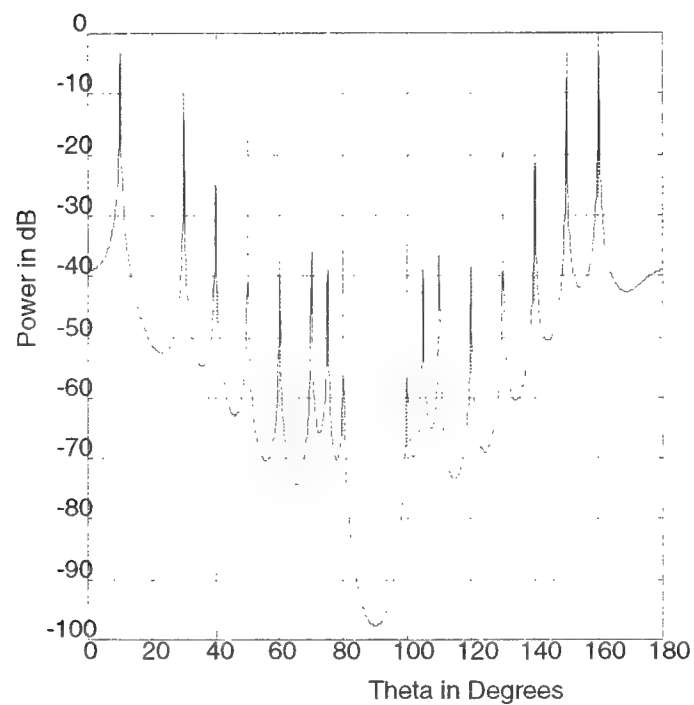


Figure 17. The RNS antenna response for $N = 13$, $L = 18$ and $N_{\max} = 16$.

Example 3:

The number of elements is $N = 17$ and the length of the array $L = 24$. Table 11 shows the three bases and element locations. Table 12 shows a comparison of the redundancy ratio and the number of received emitters for the RNS and the optimum arrays.

| Location | $N_1 = 2$ | $N_2 = 3$ | $N_3 = 4$ | Element Position |
|----------|-----------|-----------|-----------|------------------|
| $0d$ | 0 | 0 | 0 | * |
| $1d$ | 1 | 1 | 1 | |
| $2d$ | 0 | 2 | 2 | * |
| $3d$ | 1 | 0 | 3 | * |
| $4d$ | 0 | 1 | 0 | * |
| $5d$ | 1 | 2 | 1 | |
| $6d$ | 0 | 0 | 2 | * |
| $7d$ | 1 | 1 | 3 | |
| $8d$ | 0 | 2 | 0 | * |
| $9d$ | 1 | 0 | 1 | * |
| $10d$ | 0 | 1 | 2 | * |
| $11d$ | 1 | 2 | 3 | |
| $12d$ | 0 | 0 | 0 | * |
| $13d$ | 1 | 1 | 1 | |
| $14d$ | 0 | 2 | 2 | * |
| $15d$ | 1 | 0 | 3 | * |
| $16d$ | 0 | 1 | 0 | * |
| $17d$ | 1 | 2 | 1 | |
| $18d$ | 0 | 0 | 2 | * |
| $19d$ | 1 | 1 | 3 | |
| $20d$ | 0 | 2 | 0 | * |
| $21d$ | 1 | 0 | 1 | * |
| $22d$ | 0 | 1 | 2 | * |
| $23d$ | 1 | 2 | 3 | |
| $24d$ | 0 | 0 | 0 | * |

Table 11. Element positioning in an array using 3 bases
($N_1 = 2, N_2 = 3, N_3 = 4$).

| Array Type | R_r | N_{\max} |
|-------------|-------|------------|
| RNS | 6.18 | 22 |
| Optimum MRA | 5.67 | 24 |

Table 12. Comparison for example 3.

The antenna responses for the RNS and optimum cases are shown in Figure 18 and Figure 19 respectively. They are the responses for 24 emitters. The emitter directions are 20, 30, 40, 45, 50, 60, 65, 70, 75, 80, 85, 90, 95, 100, 105, 110, 115, 120, 125, 130, 140, 150, 160, and 178.

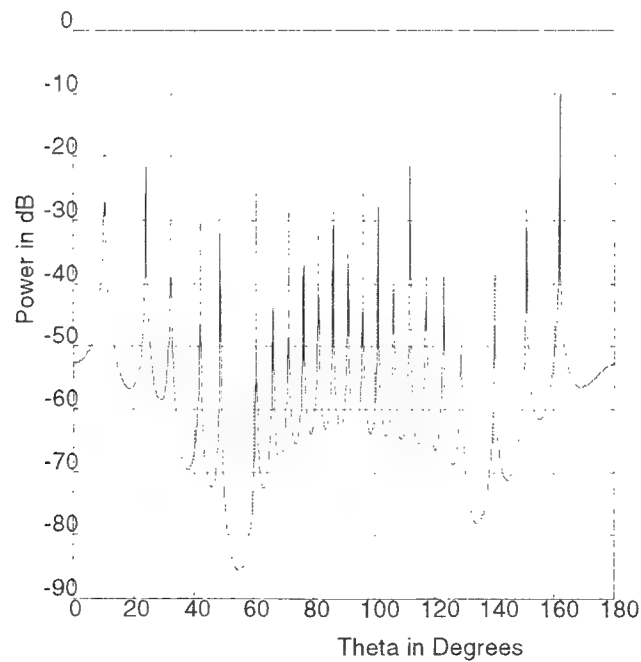


Figure 18. The RNS antenna response for $N = 17$, $L = 24$.

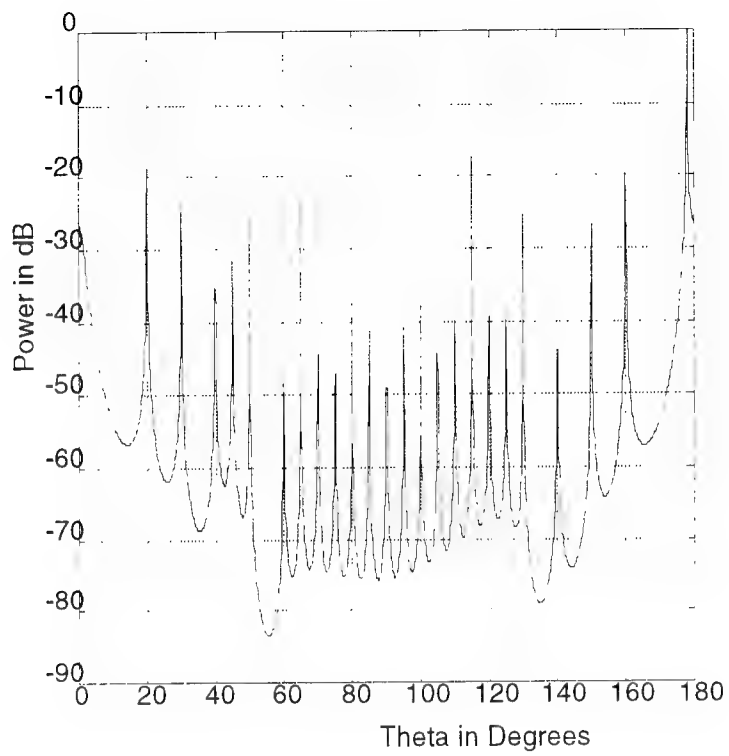


Figure 19. The optimum antenna response for $N = 17$, $L = 24$.

Figure 20 is a plot of the RNS antenna response for its maximum number of received emitters $N_{\max} = 22$. The new emitter directions are 10, 25, 30, 40, 50, 60, 65, 70, 75, 80, 85, 90, 95, 100, 105, 110, 120, 125, 130, 140, 150 and 160 degrees.

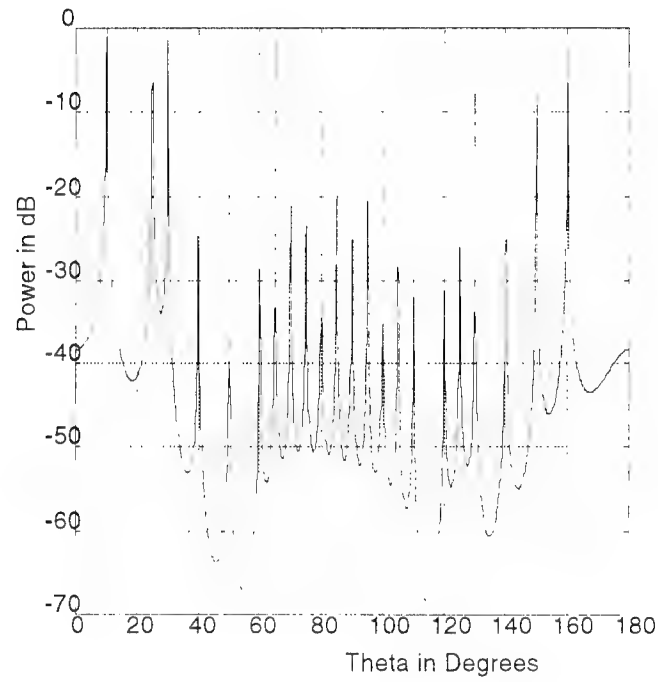


Figure 20. The RNS antenna response for $N = 17$, $L = 24$ and $N_{\max} = 22$.

Example 4:

The number of elements is $N = 23$ and the length of the array $L = 30$. Table 13 shows the three bases and the element locations. Table 14 shows a comparison of the redundancy ratio and the number of received emitters for the RNS and the optimum arrays.

| Location | $N_1 = 2$ | $N_2 = 3$ | $N_3 = 5$ | Element Position |
|----------|-----------|-----------|-----------|------------------|
| $0d$ | 0 | 0 | 0 | * |
| $1d$ | 1 | 1 | 1 | |
| $2d$ | 0 | 2 | 2 | * |
| $3d$ | 1 | 0 | 3 | * |
| $4d$ | 0 | 1 | 4 | * |
| $5d$ | 1 | 2 | 0 | * |
| $6d$ | 0 | 0 | 1 | * |
| $7d$ | 1 | 1 | 2 | |
| $8d$ | 0 | 2 | 3 | * |
| $9d$ | 1 | 0 | 4 | * |
| $10d$ | 0 | 1 | 0 | * |
| $11d$ | 1 | 2 | 1 | |
| $12d$ | 0 | 0 | 2 | * |
| $13d$ | 1 | 1 | 3 | |
| $14d$ | 0 | 2 | 4 | * |
| $15d$ | 1 | 0 | 0 | * |
| $16d$ | 0 | 1 | 1 | * |
| $17d$ | 1 | 2 | 2 | |
| $18d$ | 0 | 0 | 3 | * |
| $19d$ | 1 | 1 | 4 | |
| $20d$ | 0 | 2 | 0 | * |
| $21d$ | 1 | 0 | 1 | * |
| $22d$ | 0 | 1 | 2 | * |
| $23d$ | 1 | 2 | 3 | |
| $24d$ | 0 | 0 | 4 | * |
| $25d$ | 1 | 1 | 0 | * |
| $26d$ | 0 | 2 | 1 | * |
| $27d$ | 1 | 0 | 2 | * |
| $28d$ | 0 | 1 | 3 | * |
| $29d$ | 1 | 2 | 4 | |
| $30d$ | 0 | 0 | 0 | * |

Table 13. Element positioning in an array using 3 bases
($N_1 = 2, N_2 = 3, N_3 = 5$)

| Array Type | R_r | N_{\max} |
|-------------|-------|------------|
| RNS | 9.03 | 28 |
| Optimum MRA | 8.43 | 30 |

Table 14. Comparison for example 4.

The antenna responses for the RNS case and the optimum case are shown in Figure 21 and Figure 22 respectively. The emitter directions are 5, 15, 30, 35, 40, 45, 50, 55, 60, 65, 70, 75, 80, 85, 90, 95, 100, 105, 110, 115, 120, 125, 130, 135, 140, 145, 150, 155, 165 and 178.

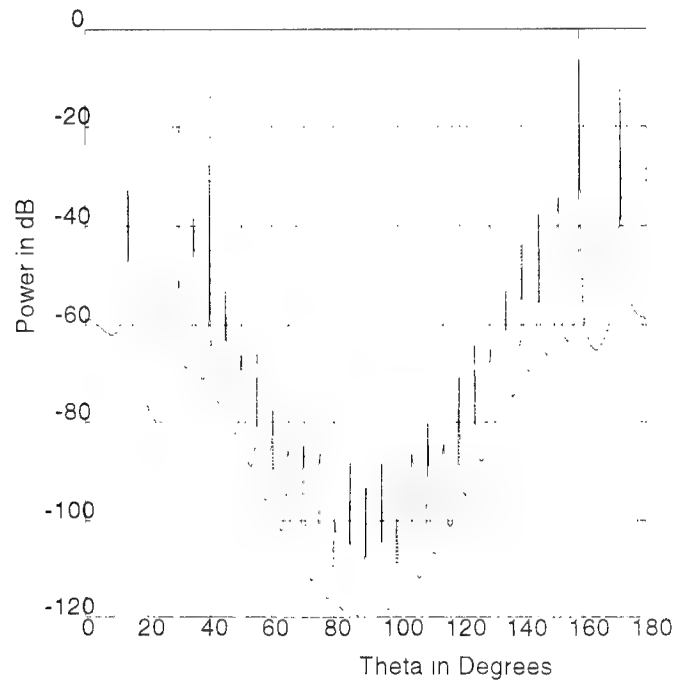


Figure 21. The RNS antenna response for $N = 23$, $L = 30$.

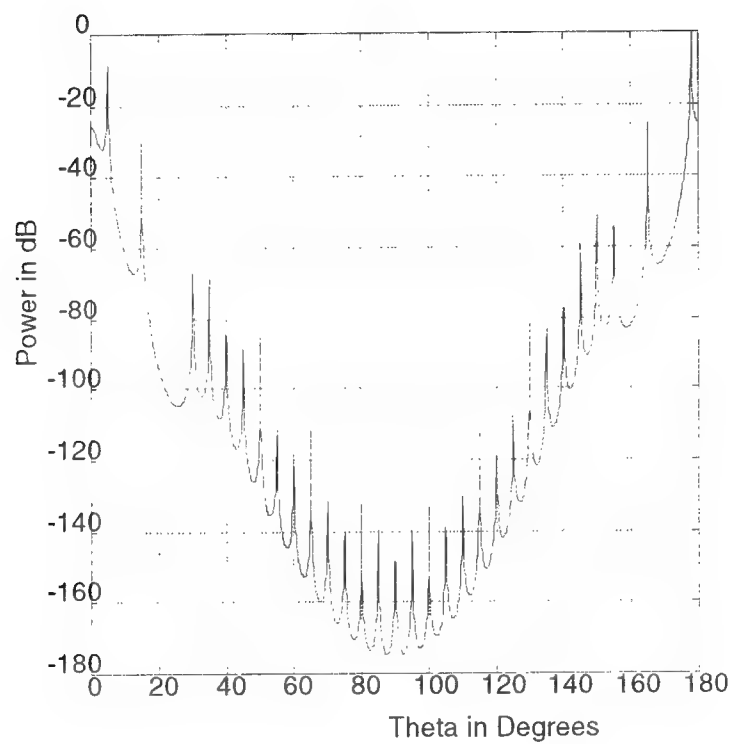


Figure 22. The optimum antenna response for $N = 23$, $L = 30$.

Figure 23 is a plot of the RNS antenna response for its maximum number of received emitters $N_{\max}=28$. The new emitter directions are 10, 20, 35, 40, 45, 50, 55, 60, 65, 70, 75, 80, 85, 90, 95, 100, 105, 110, 115, 120, 125, 130, 135, 140, 145, 150, 160 and 170 degrees.

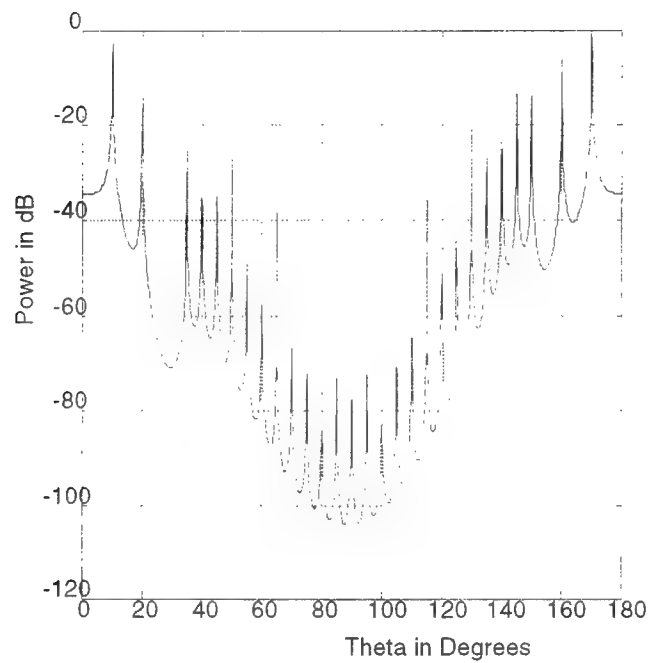


Figure 23. The RNS antenna response for $N = 23$, $L = 30$ and $N_{\max} = 28$.

Example 5:

The number of elements is $N = 19$ and the length of the array $L = 36$. Table 15 shows the three bases and the element locations. Table 16 shows a comparison of the redundancy ratio and the number of received emitters for the RNS and optimum arrays.

| Location | $N_1 = 3$ | $N_2 = 3$ | $N_3 = 4$ | Element Position |
|----------|-----------|-----------|-----------|------------------|
| $0d$ | 0 | 0 | 0 | * |
| $1d$ | 1 | 1 | 1 | |
| $2d$ | 2 | 2 | 2 | |
| $3d$ | 0 | 0 | 3 | * |
| $4d$ | 1 | 1 | 0 | * |
| $5d$ | 2 | 2 | 1 | |
| $6d$ | 0 | 0 | 2 | * |
| $7d$ | 1 | 1 | 3 | |
| $8d$ | 2 | 2 | 0 | * |
| $9d$ | 0 | 0 | 1 | * |
| $10d$ | 1 | 1 | 2 | |
| $11d$ | 2 | 2 | 3 | |
| $12d$ | 0 | 0 | 0 | * |
| $13d$ | 1 | 1 | 1 | |
| $14d$ | 2 | 2 | 2 | |
| $15d$ | 0 | 0 | 3 | * |
| $16d$ | 1 | 1 | 0 | * |
| $17d$ | 2 | 2 | 1 | |
| $18d$ | 0 | 0 | 2 | * |
| $19d$ | 1 | 1 | 3 | |
| $20d$ | 2 | 2 | 0 | * |
| $21d$ | 0 | 0 | 1 | * |
| $22d$ | 1 | 1 | 2 | |
| $23d$ | 2 | 2 | 3 | |
| $24d$ | 0 | 0 | 0 | * |
| $25d$ | 1 | 1 | 1 | |
| $26d$ | 2 | 2 | 2 | |
| $27d$ | 0 | 0 | 3 | * |
| $28d$ | 1 | 1 | 0 | * |
| $29d$ | 2 | 2 | 1 | |
| $30d$ | 0 | 0 | 2 | * |
| $31d$ | 1 | 1 | 3 | |
| $32d$ | 2 | 2 | 0 | * |
| $33d$ | 0 | 0 | 1 | * |
| $34d$ | 1 | 1 | 2 | |
| $35d$ | 2 | 2 | 3 | |
| $36d$ | 0 | 0 | 0 | * |

Table 15. Element positioning in an array using 3 bases
 $(N_1 = 3, N_2 = 3, N_3 = 4)$.

| Array Type | R_r | N_{\max} |
|-------------|-------|------------|
| RNS | 5.7 | 30 |
| Optimum MRA | 4.75 | 36 |

Table 16. Comparison for example 5.

The antenna responses for the RNS case and the optimum case are shown in Figure 24 and Figure 25 respectively. The emitter directions are 5, 10, 15, 20, 25, 30, 35, 40, 45, 50, 55, 60, 65, 70, 75, 80, 85, 90, 95, 100, 105, 110, 115, 120, 125, 130, 135, 140, 145, 150, 155, 160, 165, 170, 175 and 178 degrees.

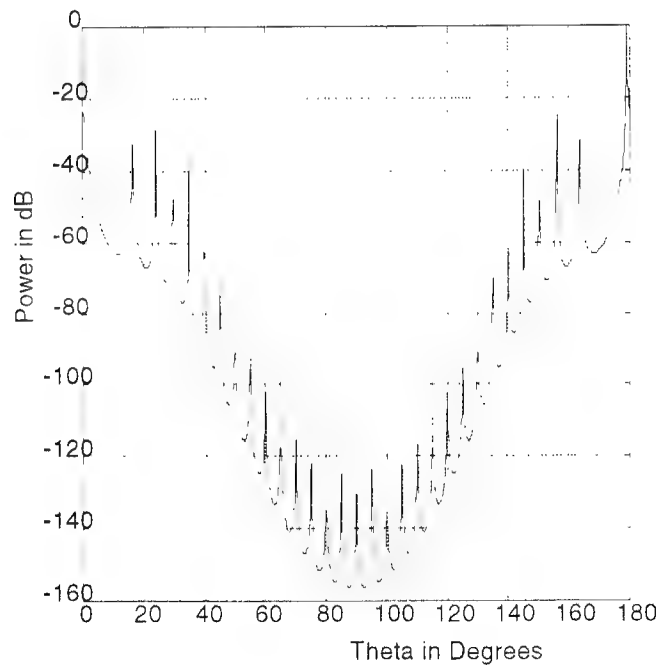


Figure 24. The RNS antenna response for $N = 19$, $L = 36$.

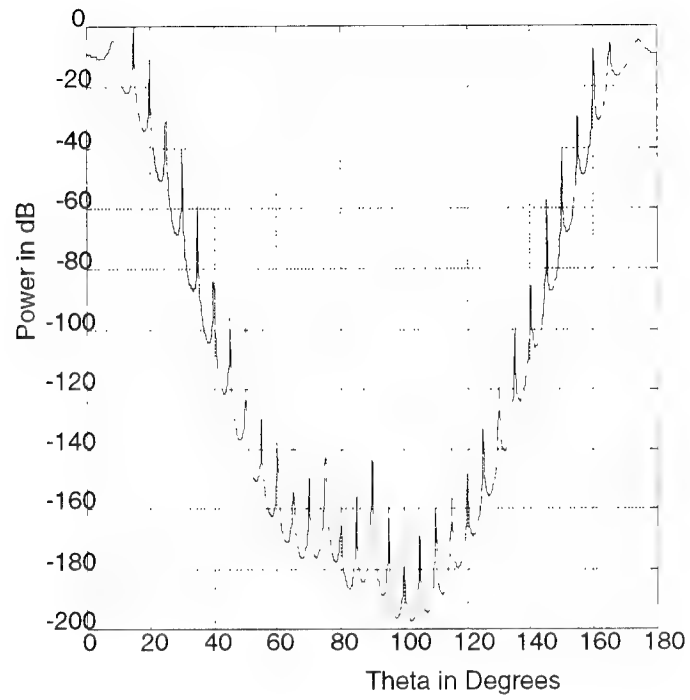


Figure 25. The optimum antenna response for $N = 19$, $L = 36$.

Figure 25 is a plot of the RNS antenna response for its maximum number of received emitters $N_{\max} = 30$. The new emitter directions are 15, 25, 30, 35, 40, 45, 50, 55, 60, 65, 70, 75, 80, 85, 90, 95, 100, 105, 110, 115, 120, 125, 135, 140, 145, 150, 155, 165 and 178 degrees.

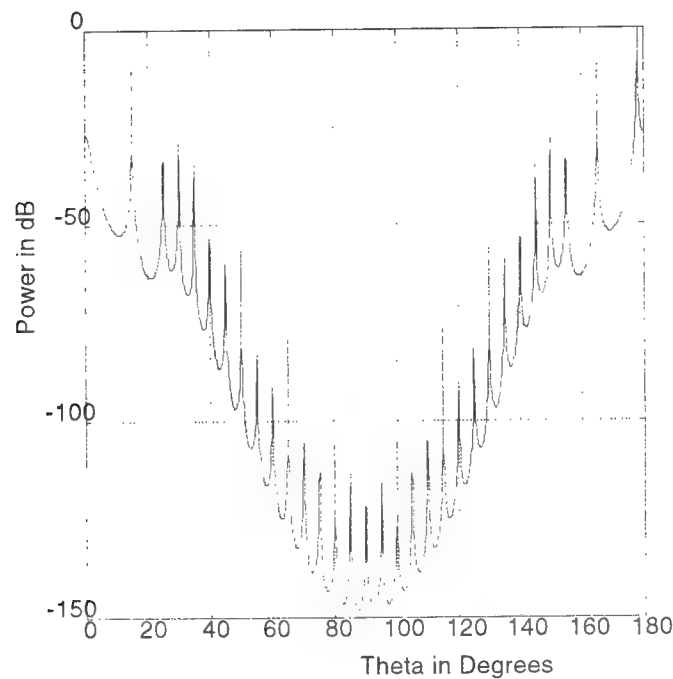


Figure 26. The RNS antenna response for $N = 19$, $L = 36$ and $N_{\max} = 30$.

B. SUMMARY OF SIMULATION RESULTS

Example 1 shows that for a relatively small number of elements ($N < 10$) and short array lengths ($L < 16$), the optimum method is suitable since it gives a lower redundancy ratio than the RNS (3 versus 3.6) with little computational penalty (5 minutes on a Sun Sparc 10 for the MRA versus less than 1 second for the RNS array). The antenna response is similar for both arrays except that the optimum is capable of resolving two more emitters than the RNS array. When the number of elements is increased to $N = 13$ and the length of the array to $L = 18$ as in Example 2, the redundancy ratio is slightly better for the optimum (4.33 versus 4.88). However, it takes approximately 2 hours on the Sun Sparc 10 to arrive at MRA configuration while the RNS calculation is still less than 1 second. The antenna response is similar for both cases with the exception that an extra two emitters can be handled in the optimum case.

In Example 3 the number of elements is increased further to $N = 17$ and the length of the array to $L = 24$. The redundancy ratio for the optimum is 5.67 versus 6.18 for the RNS. The cpu time for the optimum redundancy solution was approximately 24 hours on the Sun Sparc 10, but less than 1 second for the RNS array. The difference in emitter responses for the optimum and the RNS is two more emitters in favor of the optimum. With the number of elements $N = 23$ and the length of the array is $L = 30$ in example 4, the redundancy ratio for the optimum case is 8.43 versus 9.03 for the RNS. It took approximately 48 hours to obtain the optimum redundancy arrangement, but only several seconds to arrive at the RNS arrangement. Once again, the difference in the antenna response is due to the two extra emitters that the optimum method can accommodate. Finally, the number of elements is reduced to $N = 19$ and the length of the array increased to $L = 36$. The redundancy ratio for the optimum is found to be 4.75. It took 96 hours to arrive at this array. The difference in the number of the received emitters is 6 in favor of the optimum, hence, the difference in the antenna response.

Appendix B contains a table of additional values of R_r , N_{\max} , and L for a wide range of RNS bases taken in combinations of three.

V. CONCLUSIONS AND RECOMMENDATIONS

The important parameters used to establish the effectiveness of low redundancy arrays are the number of elements, N , the number of emitters that can be resolved, N_{\max} , and the length of the array, L . The previous chapter has shown that determining the optimum configuration is computationally intensive and not practical for large numbers of elements.

In this thesis, a method was described that uses residue number systems to generate element locations for a linear aperiodic array which increases the array's direction finding capability well beyond the conventional limit of $N-1$. The RNS redundancy ratio compares favorably to that of the optimum MRA and is capable of resolving nearly as many received emitters as the optimum. The RNS array design processing time is negligible and the arrays are easily determined for large numbers of elements and long baselines.

In order for any array to be able to detect N_{\max} emitters, the covariance matrix should have $0d, 1d, 2d, \dots, N_{\max}d$ with no integer multiple missing. For example an array with elements located at $0, 1d, 2d, 3d, 4d, 6d, 7d$ has $5d$ missing, which implies $N_{\max} = 4$. Thus, if N_{\max} does not include at least a $1d$ then $N_{\max} = 0$ and the redundancy ratio is $N(N-1)/2N_{\max} = \infty$. This is the origin of the infinities in Appendix B.

The data in Appendix B does not give any indication that an optimum RNS array exists. As the bases N_1, N_2 , and N_3 are increased, the length, N_{\max} , and R_r also increase. The values of these parameters are always superior to those for the periodic array, but inferior to those for the optimum MRA. At this point it is not clear if the moderate decrease in R_r warrants the accompanying increase in beamforming network complexity and other practical design considerations. These questions should be addressed in future research.

It was noted earlier that periodic patterns of subarrays are present in RNS arrays especially when small bases are present. There is also symmetry in the element locations with respect to the center of the array. Therefore it may be possible to replace subarrays

containing the basic repetitive pattern with a single element, yet still maintain the presence of all integer multiples of d . This possibility should be investigated in future research.

APPENDIX A. COMPUTER CODES

```
% Program 1.
% This program 'test.m' computes the optimum array configuration. The required
% inputs are the number of array elements N and the length of the array M.

clear
whitebg
global N
global M
global NNmax
N=input('What is the number of array elements?')
M=input('What is the distance between the first and the last elements?')
qs=input('Do you want to test a special arrangement?','s')
if qs=='y'
dr=input('What is this arrangement')
end
N0= 10^(-30/10);
Ns=12;
theta=[20 35 50 60 70 80 100 110 120 130 145 165];
Ps=[1,1,1,1,1,1,1,1,1,1,1,1];
minred1
i=sqrt(-1);
for k1=0:NNmax
for k2=0:NNmax
if k1==k2
R(k1+1,k2+1)=N0;
else
R(k1+1,k2+1)=0;
end
for k3=1:Ns
R(k1+1,k2+1)=R(k1+1,k2+1)+Ps(k3)*exp(-i*pi*(k1-k2)*cos(theta(k3)*pi/180));
end
end
end
[E,L]=eig(R);
clg
ee=[];
[l1,l2]=sort(abs(diag(L)));
plot(flipud(l1)),grid;
ns=input('what is the dimension of the noise space?')
for ke=1:ns
ee=[ee,E(:,l2(ke))] ;
```

```

end
w=linspace(0,pi,1200);
for k2=1:1200
for k1=1:NNmax+1
Sh(k1,1)=exp(i*pi*(k1-1)*cos(w(k2)));
end
ss=conj((ee'))*Sh;
y(k2)=1/(ss'*ss);
end
plot(180*w/pi,10*log10(y/max(y)),'-'),grid
xlabel('Theta in Degrees')
ylabel('Power in Degrees')
if qs=='y'
testmat=zeros(N*(N-1)/2,1);
for i=1:N
for j=i+1:N
testmat(dr(j)-dr(i))=1;
end
end
prod=1;
for i=1:N*(N-1)/2
prod=prod*testmat(i);
if prod==0
Nr=i-1
Rr=N*(N-1)/(2*Nr)
break
end
end
end
end

```

```
% Program 2.
% This program 'minred1.m' calculates the minimum redundancy configuration
% for a given N and M as given in the main program test.m.
```

```
global d
global N,
global M
global uplim
global Nmax
global NNmax
global dminred
NNmax=-10000;
d=[];
clear lowlim;
n=N-2;
d(1)=0;
d(N)=M;
for i=1:N-2
    lowlim(i)=i;
    uplim(i)=M-(N-(1+i));
end
d=[d(1) lowlim d(N)]
incr1(2);
Rmin=N*(N-1)/(2*NNmax)
dminred
```

```
% Program 3.
% This program 'incr1.m' test the elements one at a time to check for minimality
% of the redundancy and keeps the configuration that has the minimum
% redundancy .
```

```
function incr(ind)
global d,
global N,
global M,
global uplim
global testmat
global Nmax
global NNmax
global dminred
if ind<=(N-1)
ml=d(ind-1)+1;
mup=uplim(ind-1);
for i=ml:mup
d(ind)=i;
incr1(ind+1)
end
end
if (ind==N)
testmat=zeros(N*(N-1)/2,1);
for i=1:N-1
for j=i+1:N
testmat(d(j)-d(i))=1;
end
end
prod=1;
for i=1:N*(N-1)/2
prod=prod*testmat(i);
if testmat(i)==0
Nmax=i-1;
if(Nmax>=NNmax)
NNmax=Nmax;
dminred=d;
end
break
end
end
if prod==1
```

```
NNmax=N*(N-1)/2  
dminred=d  
end  
end
```

```
% Program 4.
% This program 'test111.m' does the same operation as that of 'test.m' except
% that the element configuration comes from the modulo combination which is
% provided by 'mod0test' program.
```

```
clear
whitebg
global N
global M
global NNmax
test000
N0= 10^(-30/10);
Ns=36;
theta=[5;10;15;20;25;30;35;40;45;50;55;60;65;70;75;80;85;90;95;100;105;110;1
15;120;125;130;135;140;145;150;155;160;165;170;175;178];
Ps=[1,1,1,1,1,1,1,1,1,1,1,1,1,1,1,1,1,1,1,1,1,1,1,1,1,1,1,1,1,1,1,1];
i=sqrt(-1);
for k1=0:NNmax
for k2=0:NNmax
if k1==k2
R(k1+1,k2+1)=N0;
else
R(k1+1,k2+1)=0;
end
for k3=1:Ns
R(k1+1,k2+1)=R(k1+1,k2+1)+Ps(k3)*exp(-i*pi*(k1-k2)*cos(theta(k3)*pi/180));
end
end
end
[E,L]=eig(R);
clg
ee=[];
[l1,l2]=sort(abs(diag(L)));
plot(flipud(l1)),grid;
ns=input('what is the dimension of the noise space?')
for ke=1:ns
ee=[ee,E(:,l2(ke))] ;
end
w=linspace(0,pi,1200);
for k2=1:1200
for k1=1:NNmax+1
```

```

Sh(k1,1)=exp(i*pi*(k1-1)*cos(w(k2)));
end
ss=conj((ee'))*Sh;
y(k2)=1/(ss*ss);
end
plot(180*w/pi,10*log10(y/max(y)),'-'),grid
xlabel('Theta in Degrees')
ylabel('Power in dB')

```



```
% Program 5.  
% This program 'test000.m' calculate the redundancy ratio and the maximum  
% number of received emitters for the modulo method.
```

```
global N  
global M  
global NNmax  
mod0test  
N=max(size(dr));  
M=dr(N)-dr(1);  
for i=1:N  
    for j=i+1:N  
        testmat(dr(j)-dr(i))=1;  
    end  
end  
prod=1;  
for i=1:max(size(testmat))  
    prod=prod*testmat(i);  
    if prod==0  
        NNmax=i-1  
        Rr=N*(N-1)/(2*NNmax)  
        break  
    end  
end
```

```
% Program 6.  
% This program 'mod0test.m' determines the element location using the  
% modulo method to use with 'test111.m'.
```

```
N1=input('what is the spacing N1?')  
N2= input('what is the spacing N2?')  
N3=input('what is the spacing N3?')  
Nsize=N1*N2*N3+1;  
v1=zeros(1,Nsize);  
v2=v1;  
v3=v1;  
dr=[];  
for i=1:Nsize  
v1(i)=rem(i-1,N1);  
v2(i)=rem(i-1,N2);  
v3(i)=rem(i-1,N3);  
if (v1(i)==0)|(v2(i)==0)|(v3(i)==0);  
dr=[dr (i-1)];  
end  
end
```


APPENDIX B. RESIDUE ARRAY PERFORMANCE DATA

This appendix contains residue array performance data for three bases ($N_1 = 2, 3, \dots, 15$; $N_2 = 3, 4, \dots, 16$; $N_3 = 3$). It gives the redundancy ratio of the residual array to that of the periodic array (R_r/R_p), the number of elements N , and the length of the array L in fundamental spacing units d .

| N_1 | | 2 | 3 | 4 | 5 | 6 | 7 | 8 |
|-------|----------|---------|----------|----------|----------|----------|----------|----------|
| N_2 | ratio | 0.5417 | ∞ | 0.3167 | 0.2775 | ∞ | 0.2353 | 0.2227 |
| 3 | elements | 13.0000 | 10.0000 | 19.0000 | 22.0000 | 19.0000 | 28.0000 | 31.0000 |
| | L | 18.0000 | 27.0000 | 36.0000 | 45.0000 | 54.0000 | 63.0000 | 72.0000 |
| 4 | ratio | 0.5152 | 0.3167 | 0.2976 | 0.3895 | 0.2803 | 0.3590 | 0.2722 |
| | elements | 17.0000 | 19.0000 | 25.0000 | 37.0000 | 37.0000 | 49.0000 | 49.0000 |
| | L | 24.0000 | 36.0000 | 48.0000 | 60.0000 | 72.0000 | 84.0000 | 96.0000 |
| 5 | ratio | 0.6024 | 0.2775 | 0.3895 | 0.2507 | 0.2447 | 0.3149 | 0.3095 |
| | elements | 23.0000 | 22.0000 | 37.0000 | 36.0000 | 43.0000 | 58.0000 | 65.0000 |
| | L | 30.0000 | 45.0000 | 60.0000 | 75.0000 | 90.0000 | 105.0000 | 120.0000 |
| 6 | ratio | 0.4902 | ∞ | 0.2803 | 0.2447 | ∞ | 0.2068 | 0.1955 |
| | elements | 25.0000 | 19.0000 | 37.0000 | 43.0000 | 37.0000 | 55.0000 | 61.0000 |
| | L | 36.0000 | 54.0000 | 72.0000 | 90.0000 | 108.0000 | 126.0000 | 144.0000 |
| 7 | ratio | 0.5536 | 0.2353 | 0.3590 | 0.3149 | 0.2068 | 0.2032 | 0.2623 |
| | elements | 31.0000 | 28.0000 | 49.0000 | 58.0000 | 55.0000 | 64.0000 | 85.0000 |
| | L | 42.0000 | 63.0000 | 84.0000 | 105.0000 | 126.0000 | 147.0000 | 168.0000 |
| 8 | ratio | 0.4783 | 0.2227 | 0.2722 | 0.3095 | 0.1955 | 0.2623 | 0.1896 |
| | elements | 33.0000 | 31.0000 | 49.0000 | 65.0000 | 61.0000 | 85.0000 | 81.0000 |
| | L | 48.0000 | 72.0000 | 96.0000 | 120.0000 | 144.0000 | 168.0000 | 192.0000 |
| 9 | ratio | 0.4744 | ∞ | 0.2696 | 0.2352 | ∞ | 0.1985 | 0.1877 |
| | elements | 37.0000 | 28.0000 | 55.0000 | 64.0000 | 55.0000 | 82.0000 | 91.0000 |
| | L | 54.0000 | 81.0000 | 108.0000 | 135.0000 | 162.0000 | 189.0000 | 216.0000 |
| 10 | ratio | 0.4713 | 0.2056 | 0.3041 | 0.2333 | 0.1802 | 0.2527 | 0.2273 |
| | elements | 41.0000 | 37.0000 | 65.0000 | 71.0000 | 73.0000 | 103.0000 | 113.0000 |
| | L | 60.0000 | 90.0000 | 120.0000 | 150.0000 | 180.0000 | 210.0000 | 240.0000 |
| 11 | ratio | 0.5118 | 0.1995 | 0.3160 | 0.2822 | 0.1748 | 0.2424 | 0.2348 |
| | elements | 47.0000 | 40.0000 | 73.0000 | 86.0000 | 79.0000 | 112.0000 | 125.0000 |
| | L | 66.0000 | 99.0000 | 132.0000 | 165.0000 | 198.0000 | 231.0000 | 264.0000 |
| 12 | ratio | 0.4667 | ∞ | 0.2645 | 0.2306 | ∞ | 0.1946 | 0.1840 |
| | elements | 49.0000 | 37.0000 | 73.0000 | 85.0000 | 73.0000 | 109.0000 | 121.0000 |
| | L | 72.0000 | 108.0000 | 144.0000 | 180.0000 | 216.0000 | 252.0000 | 288.0000 |
| 13 | ratio | 0.5010 | 0.1902 | 0.3051 | 0.2715 | 0.1667 | 0.2354 | 0.2223 |
| | elements | 55.0000 | 46.0000 | 85.0000 | 100.0000 | 91.0000 | 130.0000 | 145.0000 |
| | L | 78.0000 | 117.0000 | 156.0000 | 195.0000 | 234.0000 | 273.0000 | 312.0000 |
| 14 | ratio | 0.4634 | 0.1867 | 0.2878 | 0.2674 | 0.1635 | 0.1930 | 0.2150 |
| | elements | 57.0000 | 49.0000 | 89.0000 | 107.0000 | 97.0000 | 127.0000 | 153.0000 |
| | L | 84.0000 | 126.0000 | 168.0000 | 210.0000 | 252.0000 | 294.0000 | 336.0000 |
| 15 | ratio | 0.4621 | ∞ | 0.2615 | 0.2280 | ∞ | 0.1924 | 0.1818 |
| | elements | 61.0000 | 46.0000 | 91.0000 | 106.0000 | 91.0000 | 136.0000 | 151.0000 |
| | L | 90.0000 | 135.0000 | 180.0000 | 225.0000 | 270.0000 | 315.0000 | 360.0000 |
| 16 | ratio | 0.4610 | 0.1809 | 0.2608 | 0.2608 | 0.1584 | 0.2250 | 0.1813 |
| | elements | 65.0000 | 55.0000 | 97.0000 | 121.0000 | 109.0000 | 157.0000 | 161.0000 |
| | L | 96.0000 | 144.0000 | 192.0000 | 240.0000 | 288.0000 | 336.0000 | 384.0000 |

| N_1 | | 9 | 10 | 11 | 12 | 13 | 14 | 15 |
|------------|----------|----------|----------|----------|----------|----------|----------|----------|
| N_2 3 | ratio | ∞ | 0.2056 | 0.1995 | ∞ | 0.1902 | 0.1867 | ∞ |
| | elements | 28.0000 | 37.0000 | 40.0000 | 37.0000 | 46.0000 | 49.0000 | 46.0000 |
| | L | 81.0000 | 90.0000 | 99.0000 | 108.0000 | 117.0000 | 126.0000 | 135.0000 |
| 4 | ratio | 0.2696 | 0.3041 | 0.3160 | 0.2645 | 0.3051 | 0.2878 | 0.2615 |
| | elements | 55.0000 | 65.0000 | 73.0000 | 73.0000 | 85.0000 | 89.0000 | 91.0000 |
| | L | 108.0000 | 120.0000 | 132.0000 | 144.0000 | 156.0000 | 168.0000 | 180.0000 |
| 5 | ratio | 0.2352 | 0.2333 | 0.2822 | 0.2306 | 0.2715 | 0.2674 | 0.2280 |
| | elements | 64.0000 | 71.0000 | 86.0000 | 85.0000 | 100.0000 | 107.0000 | 106.0000 |
| | L | 135.0000 | 150.0000 | 165.0000 | 180.0000 | 195.0000 | 210.0000 | 225.0000 |
| 6 | ratio | ∞ | 0.1802 | 0.1748 | ∞ | 0.1667 | 0.1635 | ∞ |
| | elements | 55.0000 | 73.0000 | 79.0000 | 73.0000 | 91.0000 | 97.0000 | 91.0000 |
| | L | 162.0000 | 180.0000 | 198.0000 | 216.0000 | 234.0000 | 252.0000 | 270.0000 |
| 7 | ratio | 0.1985 | 0.2527 | 0.2424 | 0.1946 | 0.2354 | 0.1930 | 0.1924 |
| | elements | 82.0000 | 103.0000 | 112.0000 | 109.0000 | 130.0000 | 127.0000 | 136.0000 |
| | L | 189.0000 | 210.0000 | 231.0000 | 252.0000 | 273.0000 | 294.0000 | 315.0000 |
| 8 | ratio | 0.1877 | 0.2273 | 0.2348 | 0.1840 | 0.2223 | 0.2150 | 0.1818 |
| | elements | 91.0000 | 113.0000 | 125.0000 | 121.0000 | 145.0000 | 153.0000 | 151.0000 |
| | L | 216.0000 | 240.0000 | 264.0000 | 288.0000 | 312.0000 | 336.0000 | 360.0000 |
| 9 | ratio | ∞ | 0.1730 | 0.1678 | ∞ | 0.1600 | 0.1569 | ∞ |
| | elements | 82.0000 | 109.0000 | 118.0000 | 109.0000 | 136.0000 | 145.0000 | 136.0000 |
| | L | 243.0000 | 270.0000 | 297.0000 | 324.0000 | 351.0000 | 378.0000 | 405.0000 |
| 10 | ratio | 0.1730 | 0.1716 | 0.2138 | 0.1696 | 0.2099 | 0.1986 | 0.1676 |
| | elements | 109.0000 | 121.0000 | 151.0000 | 145.0000 | 175.0000 | 185.0000 | 181.0000 |
| | L | 270.0000 | 300.0000 | 330.0000 | 360.0000 | 390.0000 | 420.0000 | 450.0000 |
| 11 | ratio | 0.1678 | 0.2138 | 0.1654 | 0.1645 | 0.2003 | 0.2008 | 0.1626 |
| | elements | 118.0000 | 151.0000 | 144.0000 | 157.0000 | 190.0000 | 203.0000 | 196.0000 |
| | L | 297.0000 | 330.0000 | 363.0000 | 396.0000 | 429.0000 | 462.0000 | 495.0000 |
| 12 | ratio | ∞ | 0.1696 | 0.1645 | ∞ | 0.1568 | 0.1538 | ∞ |
| | elements | 109.0000 | 145.0000 | 157.0000 | 145.0000 | 181.0000 | 193.0000 | 181.0000 |
| | L | 324.0000 | 360.0000 | 396.0000 | 432.0000 | 468.0000 | 504.0000 | 540.0000 |
| 13 | ratio | 0.1600 | 0.2099 | 0.2003 | 0.1568 | 0.1561 | 0.1886 | 0.1549 |
| | elements | 136.0000 | 175.0000 | 190.0000 | 181.0000 | 196.0000 | 235.0000 | 226.0000 |
| | L | 351.0000 | 390.0000 | 429.0000 | 468.0000 | 507.0000 | 546.0000 | 585.0000 |
| 14 | ratio | 0.1569 | 0.1986 | 0.2008 | 0.1538 | 0.1886 | 0.1525 | 0.1520 |
| | elements | 145.0000 | 185.0000 | 203.0000 | 193.0000 | 235.0000 | 225.0000 | 241.0000 |
| | L | 378.0000 | 420.0000 | 462.0000 | 504.0000 | 546.0000 | 588.0000 | 630.0000 |
| 15 | ratio | ∞ | 0.1676 | 0.1626 | ∞ | 0.1549 | 0.1520 | ∞ |
| | elements | 136.0000 | 181.0000 | 196.0000 | 181.0000 | 226.0000 | 241.0000 | 226.0000 |
| | L | 405.0000 | 450.0000 | 495.0000 | 540.0000 | 585.0000 | 630.0000 | 675.0000 |
| 16 | ratio | 0.1521 | 0.1960 | 0.1924 | 0.1490 | 0.1869 | 0.1779 | 0.1473 |
| | elements | 163.0000 | 209.0000 | 229.0000 | 217.0000 | 265.0000 | 281.0000 | 271.0000 |
| | L | 432.0000 | 480.0000 | 528.0000 | 576.0000 | 624.0000 | 672.0000 | 720.0000 |

LIST OF REFERENCES

1. S. U. Pillai, Y. Bar-Ness and F. Haber, "A new approach to array geometry for improved spatial spectrum estimation," *Proc. IEEE*, vol. 73, pp. 1522-1524, Oct. 1985.
2. C. Caratheodory, *Theory of functions*, Chelsea Publishing Company, New York, NY, vol. 1, Chapter 2, pp. 90-95, May 1950.
3. A. T. Moffet, "Minimum redundancy linear arrays," *IEEE Trans. on Antennas & Propagation*, vol. AP-16, pp. 172-175, March. 1968.
4. C. A. Balanis, *Antenna Theory*, John Wiley & Sons, Inc., New York, NY, Chapter 6, pp. 212-214, May 1982.
5. R. T. Compton, *Adaptive Antennas*, Prentice Hall Inc., New York, NY, Chapter 2, pp. 46-52, June 1988.
6. R. O. Schmidt, "Multiple emitter location and signal parameter estimation," *IEEE Trans. on Antennas & Propagation*, vol. AP-34, No. 3, pp. 276-280, March 1986.
7. J. Arzac, "Nouveau reseau pour l' observation radioastronomique de la brillance sur le soleil a 9350 Mc/s," *Compt. Rend. Acad. Sci (Paris)*, vol. 240, pp. 942-945, February 1955.
8. R. N. Bracewell and G. Swarup, "The Stanford microwave spectroheliograph antenna, a microsteradian pencil beam interferometer," *IRE Trans. on Antennas & Propagation*, vol. AP-9, pp. 22-30, January 1961.
9. A. E. Covington and N. W. Broten, "An interferometer for radio astronomy with a single-lobed radiation pattern," *IRE Trans. on Antennas & Propagation*, vol. AP-5, pp. 247-255, July 1957.
10. J. Leech, "On the representation of 1, 2, ..., n by differences," *J. London Math. Soc.*, vol. 31, pp. 160-169, November, 1956.
11. F. J. Taylor, "A VLSI residue arithmetic multiplier," *IEEE Trans. on Computers*, vol. C-31, No. 6, pp. 540-546, June 1982.

INITIAL DISTRIBUTION LIST

1. Defense Technical Information Center 2
Cameron Station
Alexandaria, Virginia 22304-6145
2. Library, Code 52 2
Naval Postgraduate School
Monterey, California 93943-5101
3. Chairman, Code EC 1
Department of Electrical and Computer Engineering
Naval Postgraduate School
Monterey, California 93943-5121
4. Chairman, Code EW 1
Electronic Warfare Academic Group
Naval Postgraduate School
Monterey, California 93943-5121
5. Professor David C. Jenn, Code EC/Jn 2
Department of Electrical and Computer Engineering
Naval Postgraduate School
Monterey, California 93943-5121
6. Professor Phillip E. Pace, Code EC/PC 1
Department of Electrical and Computer Engineering
Naval Postgraduate School
Monterey, California 93943-5121
7. Military Attaché 1
Embassy of the State of Bahrain
3502 International Dr. N. W.,
Washington, D. C. 20008
8. Director of Training 1
Bahrain Defence Force
P. O. Box 245
Manama, Bahrain.

9. Director of Head-Quarter Court..... 1
Bahrain Defence Force
P. O. Box 245
Manama, Bahrain.
10. Director, Training and Education 1
MCCDC, Code C46
1019 Elliot Rd.
Quantico, Virginia 22134-5027